博士論文

Functional Analysis of Cancer-associated IDH mutations

（癌関連 IDH 変異の機能についての解析）

劉　洵

LIU XUN

Contents

Contents……...….2

Abbreviations……...4

Abstract……..…….6

Introduction…….....8

Materials and Methods……..……..…….....13

Results…….24

1. Analysis of 2-HG production and cellular proliferation in MEF cells expressing cancer-associated *IDH1/2* mutations…….24

2. Identification of pathways and genes commonly regulated by cancer-associated IDH2 mutant and 2-HG…….....27

3. Identification of Glut1 as a target molecule induced by the IDH1/2 mutants and 2-HG…….....36

4. Enhanced glucose uptake and glycolysis by the IDH1/2 mutants ……..39

5. Involvement of PI3K/Akt/mTOR pathway in the regulation of Glut1 induction by cancer-associated *IDH1/2* mutations…….41

6. Involvement of Hif1α in the regulation of Glut1 by the *IDH1/2* mutations……....43

7. Involvement of the *IDH1/2* mutations in murine liver tumorigenesis…….…...45

8. Enhanced expression of Glut1 by the IDH1/2 mutants in murine liver……...…...53

Discussion……...……56

Conclusion……...……63

References……...……64

Acknowledgements……84

Abbreviations

2-HG: 2-hydroxyglutarate

α-KG: α-ketoglutarate

AML: acute myeloid leukemia

CAM: cell adhesion molecule

CCC: cholangiocarcinoma

CK19: cytokeratin-19

COX-2: cyclooxygenase-2

DN: dysplastic nodule

ECC: extrahepatic cholangiocarcinoma

Gapdh: glyceraldehyde-3-phosphate dehydrogenase

GLUT1: glucose transporter 1

GSEA: gene set enrichment analysis

HCC: hepatocellular carcinoma

Hif1α: hypoxia-inducible factor-1α

ICC: intrahepatic cholangiocarcinoma

IDH: isocitrate dehydrogenase

KDM: lysine (K)-specific demethylase

LSL: LoxP-STOP-LoxP

MEF: mouse embryonic fibroblasts

MsigDB: Molecular Signatures Database

MUT: mutant

NAD: nicotinamide adenine phosphate

NADP: nicotinamide adenine dinucleotide phosphate

PHD: prolyl hydroxylase

PI3K: phosphatidylinositol 3-kinase

ROS: reactive oxygen species

S6k: ribosomal protein S6 kinase

SLC2A1: solute carrier family 2 member 1

TCA: tricarboxylic acid

TET: ten-eleven translocation methylcytosine dioxygenase

WT: wild-type

Abstract

Isocitrate dehydrogenase 1 and 2 (*IDH1/2*) mutations and their key effector 2-hydroxyglutarate (2-HG) have been reported to promote oncogenesis in various human cancers. To elucidate molecular mechanism(s) associated with *IDH1/2* mutations, I established mouse embryonic fibroblasts (MEF) cells stably expressing cancer-associated $IDH1^{R132C}$ or $IDH2^{R172S}$ and analyzed change of metabolic characteristics of the MEF cells.

I found that IDH1/2 mutants induced intracellular 2-HG accumulation and inhibited cell proliferation in MEF cells. Expression profile analysis by RNA-seq unveiled that glucose transporter 1 (Glut1) was induced by the IDH1/2 mutants or treatment with 2-HG. Consistently, glucose uptake and glycolysis were increased by the mutants. Furthermore, PI3K/Akt/mTOR pathway and Hif1α expression were involved in the up-regulation of Glut1.

In addition, I generated mice with liver-specific expression of the IDH1 or IDH2 mutants, and investigated the development of liver tumors by crossing liver-specific *IDH1* or *IDH2* mutation knockin mice with conditional $Kras^{G12D}$ mutation knockin mice. Consequently, both *IDH1* and *IDH2* mutations enhanced oncogenic *Kras*-induced liver tumor formation, and shortened the survival of the double knockin mice. Interestingly, the *IDH1/2* mutations increased the frequency of formation of intrahepatic cholangiocarcinoma (ICC)-like tumors. Moreover, enhanced expression of Glut1 was

observed in the ICC-like lesions in the double knockin mice.

The results suggest that Glut1 is a potential target regulated by cancer-associated *IDH1/2* mutations and might be involved in the ICC development.

Introduction

Isocitrate dehydrogenases (IDHs) are metabolic enzymes that catalyze oxidative decarboxylation of isocitrate to α-ketoglutarate (α-KG) [1-3]. In humans, IDHs comprise three members including IDH1, IDH2 and IDH3, and each member has its own unique features [2-6] (Figure 1). IDH1 is located in cytosol and peroxisomes, whereas IDH2 and IDH3 are located in mitochondria[2-5]. IDH1 and IDH2 have hydrogenase activities, and generate NADPH using nicotinamide adenine dinucleotide phosphate ($NADP^+$) as electron acceptors[2-5]. IDH3 is comprised of three subunits that encoded by distinct genes (*IDH3A, IDH3B, and IDH3G*), which is involved in the generation of NADH from nicotinamide adenine dinucleotide (NAD^+) in tricarboxylic acid (TCA) cycle[2-4, 6]. These findings suggest that IDHs play a crucial role in metabolite exchange and electron transport in the mitochondria and cytosol.

Recurrent mutations of *IDH1* were initially identified in gliomas by a cancer genome sequencing project[7]. Additional studies have revealed frequent *IDH1* mutations in a variety of human cancers, including 70%~80% of low-grade gliomas[8-12], 50%~70% of chondrosarcomas[3, 10, 13, 14] and approximately 10% of acute myeloid leukemia (AML) [12, 15-18]. On the other hand, *IDH2* mutations were less frequently discovered in approximately 4% of gliomas[8, 12, 18, 19] and approximately 10% of AML[12, 16, 20-22]. It is noteworthy that *IDH1* and *IDH2* mutations were also detected in 10-20% and 2-5% of intrahepatic cholangiocarcinoma (ICC), respectively (Figure 2) [23-28]. Interestingly,

mutations in *IDH3A*, *IDH3B*, or *IDH3G* are very rare in human cancers[2, 4, 6, 29]. It is of note that *IDH1/2* mutations are usually heterozygous missense mutations, and that the mutations are primarily located at catalytic residues Arginine 132 (R132) of *IDH1* and Arginine 140 (R140) or Arginine 172 (R172) of *IDH2*[3, 5, 10, 18, 30, 31]. These mutant proteins confer a neomorphic enzymatic activity resulting in the conversion from α-KG to 2-hydroxyglutarate (2-HG) [1, 16], and the accumulated 2-HG causes extensive anomalous effects on cell homeostasis (Figure 1).

2-HG blocks cell differentiation by competitive inhibition of αKG-dependent enzymes that are involved in epigenetic regulation[32, 33], which induces additional alterations in cellular metabolism, redox state, and DNA repair[10, 11, 34-36], suggesting that 2-HG functions as a potent oncometabolite[10, 12, 37-39].

As previously mentioned, *IDH1* and *IDH2* mutations are frequently reported in human ICC[27, 40]. Cholangiocarcinoma (CCA) is the most common biliary cancer and the second most common primary hepatic malignancy[41, 42]. CCA is classified into ICC and extrahepatic cholangiocarcinoma (ECC), depending on their anatomical locations[43-45]. ICC accounts for 20% to 25% of all CCA, and its incidence and mortality have been increasing in the past few decades worldwide, representing a global health problem[44-47]. Analyses of mutations in CCA have identified frequent mutations in *KRAS*, *TP53*, *ARID1A* and *PTEN*[27, 40, 48]. Fusion gene involving *FGFR2* and mutations in *IDH1/2*, *EPHA2* and *BAP1* were characteristically identified in ICC[40]. In contrast, mutations in *IDH1* or *IDH2* are rarely detected in ECC[23, 26, 49]. *IDH1/2* mutations are reportedly

correlated with hypermethylation, poorly differentiated histology and clear cell change in ICCs [26, 50]. Conflicting results were reported in a previous study that evaluated prognosis significance in the *IDH* mutant ICC populations[51]. *IDH* mutations in ICCs have been associated with either better, worse, or unchanged overall survival[24, 28, 52]. Despite advances in the research of ICC, molecular mechanisms underlying its tumorigenesis have not been fully understood.

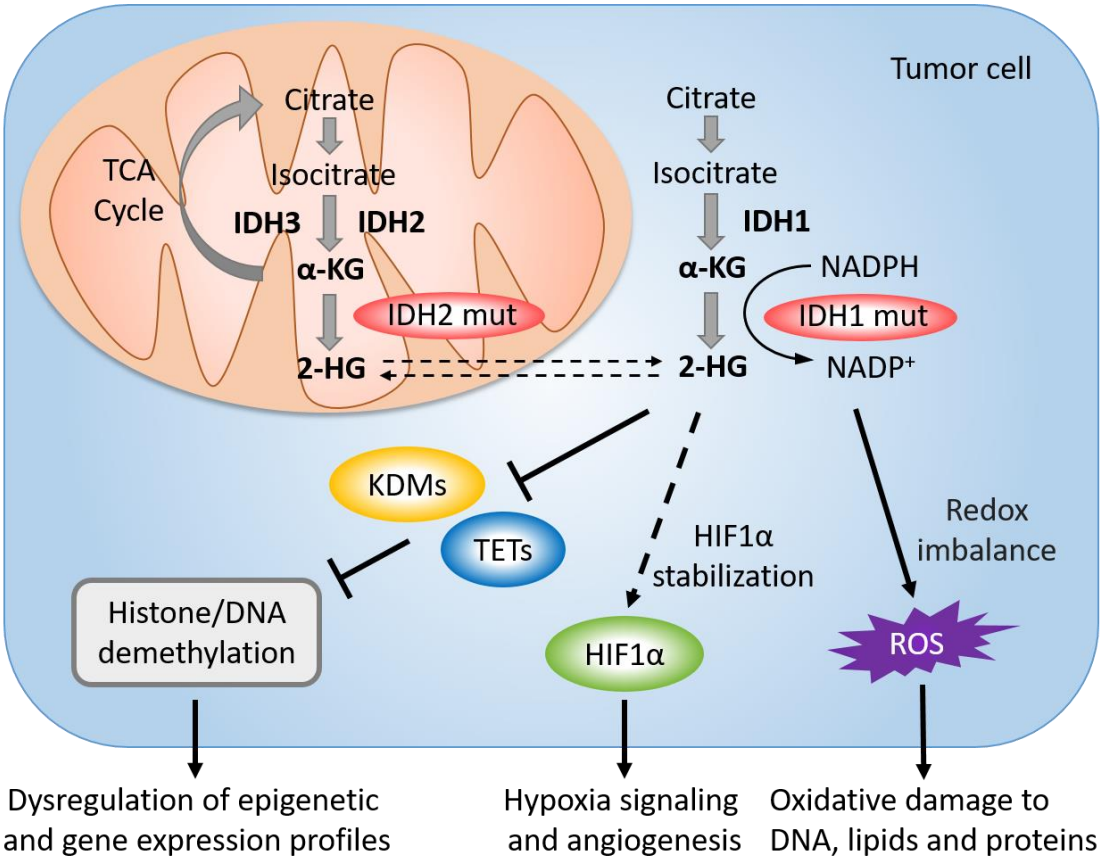

Figure 1. *IDH1/2* mutations remold the homeostasis and metabolism of cancer cells. Schematic diagram of the carcinogenesis mechanism of *IDH1/2* mutations. Mutant IDH1/2 enzymes show a neomorphic enzymatic capacity to convert α-KG into 2-HG, a small oncometabolite. The presence of mutant IDH1/2 proteins results in increased amounts of 2-HG, which then alters various downstream cellular activities. As an analog of α-KG, 2-HG serves as a competitive inhibitor for lysine (K)-specific demethylases (KDMs) or ten-eleven translocation methylcytosine dioxygenases (TETs) and therefore blocks the demethylation of histone and nucleotide, respectively. 2-HG may help to stabilize HIF1α proteins and activate hypoxia signaling pathway, which results in

increased angiogenesis in human cancer, whereas the detailed molecular mechanism of HIF1α regulation by *IDH1/2* mutations is currently unclear. The abnormal consumption of NADPH by mutant IDH1 disrupts biosynthetic reactions of reactive oxygen species (ROS) scavengers, leading to the accumulation of ROS. The elevated oxidative stress then triggers the oxidative damage in biomolecules such as DNA, lipids and proteins.

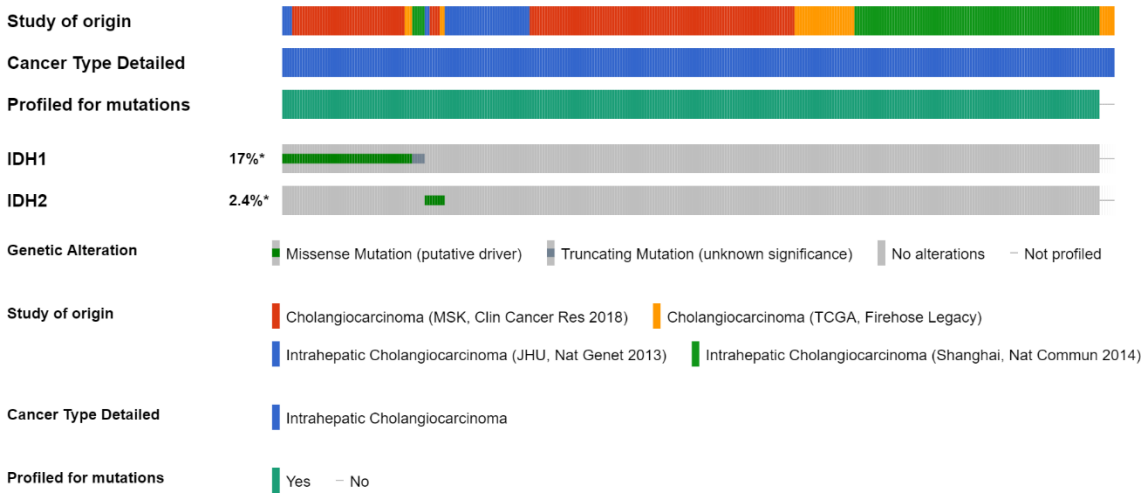

Figure 2. Frequency of *IDH1* and *IDH2* mutations in human ICC.
Frequency of *IDH1* or *IDH2* mutations in ICC was calculated using the cBioPortal for Cancer Genomics (http://www.cbioportal.org/), an open-access, open-source resource for interactive exploration of multidimensional cancer genomics database. Four independent public datasets of ICC or CCC, including "Intrahepatic Cholangiocarcinoma (Shanghai, Nat Commun 2014)"[27], "Intrahepatic Cholangiocarcinoma (JHU, Nat Genet 2013)"[28], "Cholangiocarcinoma (MSK, Clin Cancer Res 2018)"[49] and "Cholangiocarcinoma (TCGA, Firehose Legacy)", were selected. ICC cases in these datasets were analyzed simultaneously and the result was exported as an "oncoprint" automatically. Oncoprint displays the frequency of mutations, genetic alteration type, study of origin and detailed cancer type.

Altered cellular energy metabolism is one of the "hallmarks of cancer", biological characteristics acquired during carcinogenesis[53]. Two major biochemical events including increased glucose uptake and aerobic glycolysis are involved in the altered cellular energy metabolism[54]. GLUT1 encoded by the solute carrier family 2 member 1 (*SLC2A1*) gene plays a role in the uptake of glucose, and its expression is

known to be regulated by hypoxia-inducible factor-1α (HIF1α) in hypoxemic condition[55, 56]. The phosphatidylinositol 3-kinase (PI3K) /Akt signaling pathway is also reported to be associated with the regulation of GLUT1 and HIF1α expression[57-60]. Enhanced GLUT1 expression during carcinogenesis has been identified in various malignancies, such as breast, lung, and pancreatic cancer (https://www.oncomine.org), which results in increased glucose uptake into cytoplasm of tumor cells[61-63]. Elevated GLUT1 level was reportedly detected in nearly half of human ICC cases and negatively correlated with their histological differentiation, suggesting the potential role of GLUT1 in ICC carcinogenesis[64, 65].

Although the involvement of *IDH1/2* mutations in cancer has been reported, the precise mechanism(s) of mutant *IDH1/2* in carcinogenesis remains to be elucidated. In this study, I expressed cancer-associated hotspot IDH1/2 mutants in MEF cells and performed functional analysis. I identified *Slc2a1* as a novel downstream target of *IDH1/2* mutations. I also investigated the role of *IDH1/2* hotspot mutations in hepatocarcinogenesis using a conditional transgenic mouse model and found that *IDH1/2* mutations upregulated Glut1 expression and enhanced the oncogenic *Kras*-induced tumor formation in murine liver. These findings suggested that GLUT1 may be useful as a biomarker of tumors harboring *IDH1/2* mutations.

Materials and Methods

Cell culture

MEF cells were isolated from embryos of C57BL/6 mice at embryonic day 13.5 (ED13.5) and immortalized spontaneously by serial passages. MEF cells were grown in Dulbecco's modified Eagle's medium (DMEM) (Thermo Fisher Scientific, Waltham, MA) supplemented with 10% fetal bovine serum (FBS) (Thermo Fisher Scientific), and antibiotic/antimycotic solution (Sigma, St. Louis, MO).

Mice

Mice expressing Cre recombinase under the Albumin promoter (*Alb-Cre*) and mice carrying conditional knockin allele of oncogenic $Kras^{G12D}$ (LoxP-STOP-LoxP-$Kras^{G12D}$; *LSL-*$Kras^{G12D}$) were purchased from The Jackson Laboratory. The conditional knockin mice carrying human $IDH1^{R132C}$ and $IDH2^{R172S}$ (*LSL-*$IDH1^{R132C}$ and *LSL-*$IDH2^{R172S}$) were kindly provided by Dr. Makoto Hirata. In these mouse strains, coding region of mutant $IDH1^{R132C}$ or $IDH2^{R172S}$ ($IDH1/2^{mut}$) and that of EGFP were inserted in the *Rosa26* locus (Figure 3). The coding sequences of $IDH1/2^{mut}$ and *EGFP* were separated by an IRES. A polyadenylation STOP sequence flanked by two LoxP sites (an LSL-cassette) precedes $IDH1/2^{mut}$-IRES-*EGFP* cassette. Consequently, the introduction of Cre recombinase induced deletion of the LSL-cassette and expression of mutant IDH1 or IDH2 together with EGFP protein. (Figure 3). All mice were on the C57BL/6 genetic

background. PCR primers used for the genotyping of each mouse strain are listed in Table 1.

Mice were housed in specific pathogen-free conditions within the animal care facility in the Institute of Medical Science, the University of Tokyo. All of the experimental protocols were approved by the Animal Care and Use Committee of the University of Tokyo and conducted in accordance with the Guidelines for the Care and Use of Laboratory Animals of the University of Tokyo (approval nos. PA11-03 and PA16-41).

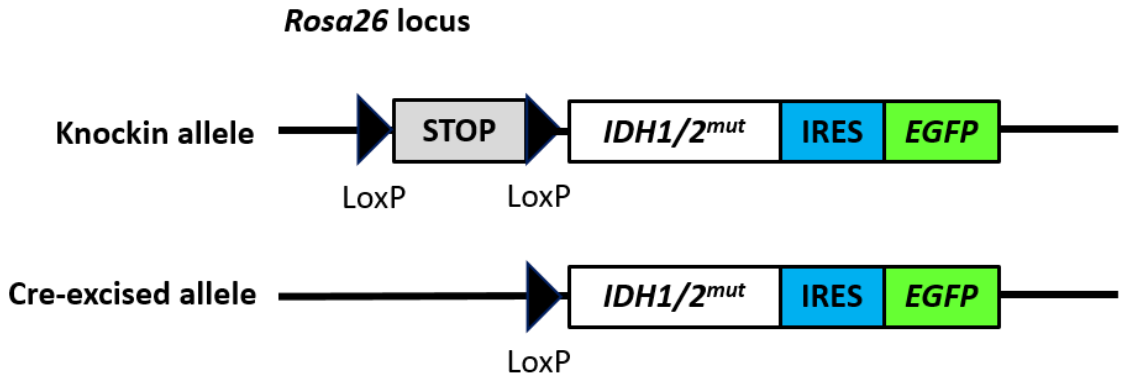

Figure 3. Generation of conditional mutant *IDH1/2* knockin mice.
Diagram of Cre recombinase mediated knockin strategy to generate *IDH1/2* mutation conditional knockin mice.

Table 1. Sequence of primers used for mouse genotyping.

Genotype	Strand	Primer Sequence (5'>3')
LSL-IDH1^{R132C}	Forward	GCTTCATCTGGGCCTGTAAA
	Reverse	GCTTTGCTCTGTGGGCTAAC
LSL-IDH2^{R172S}	Forward	TGGCTCAGGTCCTCAAGTCT
	Reverse	CTCAGCCTCAATCGTCTTCC
Alb-Cre	Forward	CCCACACTGAAATGCTCAAA
	Reverse	GAACCTCATCACTCGTTGCA
LSL-Kras^{G12D}	Forward	CCTTTACAAGCGCACGCAGACTGTAGA
	Reverse	AGCTAGCCACCATGGCTTGAGTAAGTCTGCA

Reagents

Octyl-(R)-2HG, PI-103 and rapamycin were purchased from Sigma, Cayman (Ann Arbor, MI) and LC Laboratories (Woburn, MA), respectively.

Retroviral plasmids and transduction

The wild-type (WT) cDNAs of human *IDH1* and *IDH2* were amplified by PCR using each set of gene-specific primers with cDNA of SW480 cells as a template. Sequences of the primers used are shown in Table 2. The *IDH1*^{R132C} and *IDH2*^{R172S} mutant cDNA are gifts from Dr. Makoto Hirata (National Cancer Center, Tokyo, Japan), which were generated by a PCR-based site-directed mutagenesis and the amplification using cDNA of SW1353 cells carrying the mutation as a template, respectively. Both WT and MUT *IDH1/2* cDNAs were cloned into pCAGGSn3FC vectors to fuse a 3×FLAG tag at their C-terminus. The 3×FLAG tagged WT and MUT *IDH1/2* cDNAs were subcloned into a retroviral vector pMXs to obtain wild-type and mutant pMXs-3×FLAG-IDH1/2 (pMX-IDH1WT, pMX-IDH2WT, pMX-IDH1MUT and pMX-IDH2MUT) plasmids.

Retroviral particles were produced by the transfection of 3.0×10^6 PLAT-A packaging cells with 8 μg of pMX-IDH1WT, pMX-IDH2WT, pMX-IDH1MUT, pMX-IDH2MUT or pMX-control plasmids using Fugene 6 Transfection Reagent (Promega, Madison, WI) in 100mm Collagen Type I coated Dish (Iwaki, Japan). After incubation of one day, the growth medium was changed into 5 ml for the concentration of virus. Concentrated viral supernatants were collected in 24 h and filtered through 0.45 μm filters. MEF cells were then infected with all 5 ml of fresh viral supernatant in the presence of 8 μg/ml polybrene (final concentration) and 5 ml of complete medium was added eight hours later. Two days after the infection, the cells expressing each gene were split 1:10 and maintained with selection medium containing 2 μg/ml puromycin (final concentration). After resistant MEF cells to puromycin were selected, the cells stably expressing wild-type or mutant IDH1/2 (MEF-1WT, MEF-2WT, MEF-1MUT, and MEF-2MUT) and the cells transduced with control retrovirus (control MEF) were used for experiments.

Table 2. Primers for cloning.

Plasmid vector	Strand	Enzyme	Primer Sequence (5'>3')
pCAGGSn3FC-IDH1	Forward	*Eco*RI	CCGGAATTCACCATGTCCAAAAAAA TCAGTGG
	Reverse	*Xho*I	CCGCTCGAGAAGTTTGGCCTGAGCT AGTTTG
pCAGGSn3FC-IDH2	Forward	*Eco*RI	CCGGAATTCACCATGGCCGGCTACCT GCGGGTC
	Reverse	*Xho*I	CCGCTCGAGCTGCCTGCCCAGGGCT CTGT
pMX-3FCIDH	Reverse	*Not*I	AAGGAAAAAAGCGGCCGCCTACTTG TCATCGTCATCCTTG

RNA-seq and gene set enrichment analysis

Total RNA was extracted from the stable MEF-2MUT cells, control MEF cells, and MEF cells treated with or without 2-HG using RNeasy Plus mini Kit (Qiagen, Valensia, CA). All experiments were carried out by triplicate. RNA integrity was evaluated using Agilent 2100 Bioanalyzer (Agilent Technologies, Santa Clara, CA), and RNA samples with RNA Integrity Number (RIN) > 8.8 were subjected for RNA-seq analysis. RNA-seq libraries were prepared using 100 ng of total RNA with an Ion AmpliSeq Transcriptome Mouse Gene Expression kit (Thermo Fisher Scientific), which is designed for targeted amplification of over 20,000 distinct murine gene transcripts simultaneously in a single primer pool. The libraries were sequenced on Ion Proton system using an Ion PI Hi-Q Sequencing 200 kit and Ion PI Chip v3 (Thermo Fisher Scientific), and the sequencing reads were aligned to AmpliSeq_Mouse_Transcriptome_V1_Reference using Torrent Mapping Alignment

Program (TMAP). The data were analyzed using AmpliSeqRNA plug-in v5.2.0.3, a Torrent Suite Software v5.2.2 (Thermo Fisher Scientific), which provides QC metrics and normalized read counts per gene. Data processing was performed using the GeneSpring GX13.1 (Agilent Technologies). Additionally, gene set enrichment analysis (GSEA) was performed using GSEA v4.1.0 for Windows with gene sets derived from hallmark collections, Pathway Interaction Database (PID) and BioCarta. KEGG pathway analysis was carried out using Molecular Signatures Database (MSigDB v7.2, http://www.broadinstitute.org/gsea/msigdb/index.jsp).

Quantitative reverse-transcription PCR (qRT-PCR)

Total RNA was extracted from cultured cells using RNeasy Plus mini Kit (Qiagen). Isolation of total RNA from mouse liver tissue samples was carried out by TRIzol reagent (Thermo Fisher Scientific). cDNA was synthesized from one μg of total RNA with Transcriptor First Strand cDNA Synthesis Kit (Roche Diagnostics GmbH, Mannheim, Germany). Quantitative PCR was performed using qPCR Kapa SYBR Fast ABI Prism Kit (Kapa Biosystems, Wilmington, MA) with sets of primers for *Ptgs2*, *Lamc2, Slc2a1* and *Hif1α* on StepOnePlus (Thermo Fisher Scientific). Sequences of the primers used are shown in Table 3. The levels of transcripts were determined by the relative standard curve method, and glyceraldehyde-3-phosphate dehydrogenase (*Gapdh*) was used as an internal control.

Table 3. Sequence of primers used in qPCR.

Gene	Strand	Primer Sequence (5'>3')
Ptgs2	Forward	GATGCTCTTCCGAGCTGTG
	Reverse	GGATTGGAACAGCAAGGATTT
Lamc2	Forward	CTGGAGATCAGCAGCGAGA
	Reverse	TGCTGTCACATTAGCTTCCAA
Slc2a1	Forward	TTACAGCGCGTCCGTTCT
	Reverse	TCCCACAGCCAACATGAG
Hif1α	Forward	CATGATGGCTCCCTTTTTCA
	Reverse	GTCACCTGGTTGCTGCAATA
Gapdh	Forward	TGTCCGTCGTGGATCTGAC
	Reverse	CCTGCTTCACCACCTTCTTG

Western blotting

Total protein was extracted from cultured cells using radioimmunoprecipitation assay (RIPA) buffer (50 mM Tris-HCl, pH8.0, 150 mM sodium chloride, 0.5% sodium deoxycholate, 0.1% sodium dodecyl sulfate, 1.0% NP-40) supplemented with the Protease Inhibitor Cocktail Set III (Calbiochem, San Diego, CA) and a phosphatase inhibitor cocktail PhosSTOP™ (Roche). Protein concentration was determined by BCA Protein Assay Kit (Thermo Fisher Scientific). Protein (30-50 μg/lane) was separated by 10% SDS-PAGE and transferred on to a PVDF membrane (GE Healthcare, Buckinghamshire, UK). After the blocking with 5% skim milk in TBS-T (Tris-buffered saline-Tween20) for 1 h, the membranes were incubated overnight with primary antibodies including anti-Flag (F3165, Sigma), anti-IDH1 (D2H1) (8137, Cell Signaling Technology, Danvers, MA), anti-IDH2 (D8E3B) (56439, Cell Signaling Technology), anti-Glut1 (ab115730, Abcam, Cambridge, UK), anti-phospho-S6k (9205, Cell Signaling Technology); anti-total-S6k (2708, Cell Signaling Technology); anti-phospho-Akt

(Ser473) (4060, Cell Signaling Technology); anti-phospho-Akt (Thr308) (13038, Cell Signaling Technology); anti-total-Akt (4681, Cell Signaling Technology); anti-Hif1α (14179, Cell Signaling Technology) and anti-β-actin (A5441, Sigma). All antibodies except anti-Glut1 (1:50,000) were diluted as 1:1000. Horseradish peroxidase-conjugated goat anti-mouse or anti-rabbit IgG (GE Healthcare) served as the secondary antibody for the ECL Detection System (GE Healthcare).

Cell proliferation assay

Cell proliferation assay was carried out by water soluble tetrazolium salts (WST)-based colorimetric method using Cell-counting kit-8 according to the manufacturer's recommendations (Dojindo, Kumamoto, Japan). Absorbance was measured at 450 nm using FLUOstar OPTIMA Microplate Reader (BMG Labtechnologies, GmbH, Germany).

2-HG measurement

An enzymatic 2-HG assay was used to determine the intracellular 2-HG concentration. Lysates of 5×10^6 MEF cells expressing wild-type or mutant IDH1/2 (MEF-1WT, MEF-2WT, MEF-1MUT, and MEF-2MUT) were collected. Intracellular 2-HG content was then measured using a D-2-HG Assay Kit (Abcam). Absorbance was measured by FLUOstar OPTIMA Microplate Reader (BMG Labtechnologies) at 450nm. D-2-HG concentrations of indicated cell lysates were calculated according to

manufacturer's instructions.

Glucose uptake assay

MEF cells expressing wild-type or mutant IDH1/2 (MEF-1WT, MEF-2WT, MEF-1MUT, and MEF-2MUT) were plated in a 12-well cell culture plate and were incubated overnight. Glucose uptake was measured by Glucose Uptake-Glo™ Assay (Promega), a non-radioactive, plate-based, homogeneous bioluminescent method for measuring glucose uptake in mammalian cells based on the detection of 2-deoxyglucose-6-phosphate (2DG6P), according to the manufacturer's protocol. Cell viability was quantified simultaneously by CellTiter-Glo® Luminescent Cell Viability Assay (Promega) for normalization.

Lactate level assay

Lysates of 2×10^4 MEF cells expressing wild-type or mutant IDH1/2 (MEF-1WT, MEF-2WT, MEF-1MUT, and MEF-2MUT), or control MEF cells were collected. Intracellular lactate levels were then measured by Lactate-Glo™ Assay (Promega), a bioluminescent assay for the detection of L-Lactate in mammalian cells based on lactate oxidation and NADH production coupling with a bioluminescent NADH detection system, according to manufacturer's protocol. Cell viability was quantified simultaneously by CellTiter-Glo® Luminescent Cell Viability Assay (Promega) for normalization.

Gene silencing

Small interfering RNA (siRNA) targeting *Hif1α* (SASI_Mm01_00070473), *Akt1* (Mm_Akt1_3533), *Akt2* (Mm_Akt2_5904), and *Akt3* (Mm_Akt3_0790) were purchased from Sigma and control siRNA (ON-TARGETplus Non-targeting Pool #D-001810-10) was from GE Dharmacon (Lafayette, CO). Target sequences of the siRNAs are shown in Table 4. MEF cells were seeded one day before the treatment with siRNA, and transfected with 10 nM of the aforementioned siRNAs using Lipofectamine RNAiMAX (Thermo Fisher Scientific). Forty-eight hours after the transfection, RNA and proteins were extracted from the cells. The silencing effect of siRNAs was evaluated by real-time qPCR and western blotting.

Table 4. Sequence of siRNA.

siRNA	Sequence
Control	ON-TARGETplus Non-targeting Control Pool #D-001810-10
Hif1α	CAAGCAACUGUCAUAUAUA
Akt1	GUGAUUCUGGUGAAAGAGA
Akt2	GAGAUGUGGUGUACCGUGA
Akt3	CUGUUAUAGAGAGAACAUU

Histology and immunohistochemistry

Liver tissues were collected from the mice upon autopsies, fixed with 10% formalin, and embedded in paraffin for sectioning. Sections (3 μm) were stained with hematoxylin and eosin. For immunohistochemistry (IHC), sections were dewaxed in xylene and hydrated by immersion in 100% ethanol and distilled water. Antigen retrieval

was performed by boiling for 10 min in 10 mM citrate solution (pH 6.0). The sections were subsequently incubated for 10 min in 3% H_2O_2-methanol for blocking endogenous peroxidase, blocked with 10% serum for one hour at room temperature, and incubated overnight at 4 °C with anti-Ck19 (1:100; TROMA-III, Developmental Studies Hybridoma Bank, Iowa City, IA), anti-GFP (1:100; 2555, Cell Signaling Technology), anti-Ki-67 (1:200; NB500-170, Novus Biologicals, Centennial, CO) and anti-Glut1 (1: 500; ab115730, Abcam). Slides were rinsed in TBS-T and peroxidase activity was detected using the EnVision+ Dual Link System-HRP (Dako, Denmark) and EnVision Detection System, Peroxidase/DAB+ (Dako). Nuclei were counterstained with hematoxylin for 1 min.

Statistical analysis

Statistical analysis was performed by Student's t-test with Benjamini-Hochberg correction for the analysis of gene expression profiles. The unpaired Student’s t-test was used for the statistical analysis of cell proliferation, qRT-PCR, glucose uptake assay, lactate level assay and ratio of liver weight to body weight in mice. The log-rank test was utilized for the statistical analysis of Kaplan-Meier survival analysis.

Results

1. Analysis of 2-HG production and cellular proliferation in MEF cells expressing cancer-associated *IDH1/2* mutations

To investigate the function of IDH1/2 mutants ($IDH1^{R132C}$ and $IDH2^{R172S}$) in carcinogenesis, I established MEF cells that stably express exogenous wild-type or mutant IDH1/2 (MEF-1WT, MEF-2WT, MEF-1MUT, and MEF-2MUT) using a retrovirus transduction system (Figure 4A). To evaluate converting activity of the mutant IDH1/2 proteins from α-KG to 2-HG, I measured 2-HG accumulation in MEF-1WT, MEF-2WT, MEF-1MUT, and MEF-2MUT using an enzymatic assay (Figure 4B). Compared with the control cells transfected with mock vector, exogenous expression of wild-type IDH1/2 reduced 2-HG accumulation. On the other hand, expression of the mutant IDH1 and IDH2 induced 2-HG accumulation by 1.40-fold and 3.45-fold compared to the control cells, respectively. These data indicate that both mutants enhance the conversion from α-KG to 2-HG, and that the mutant IDH2 has higher effect on the conversion to 2-HG compared with the mutant IDH1.

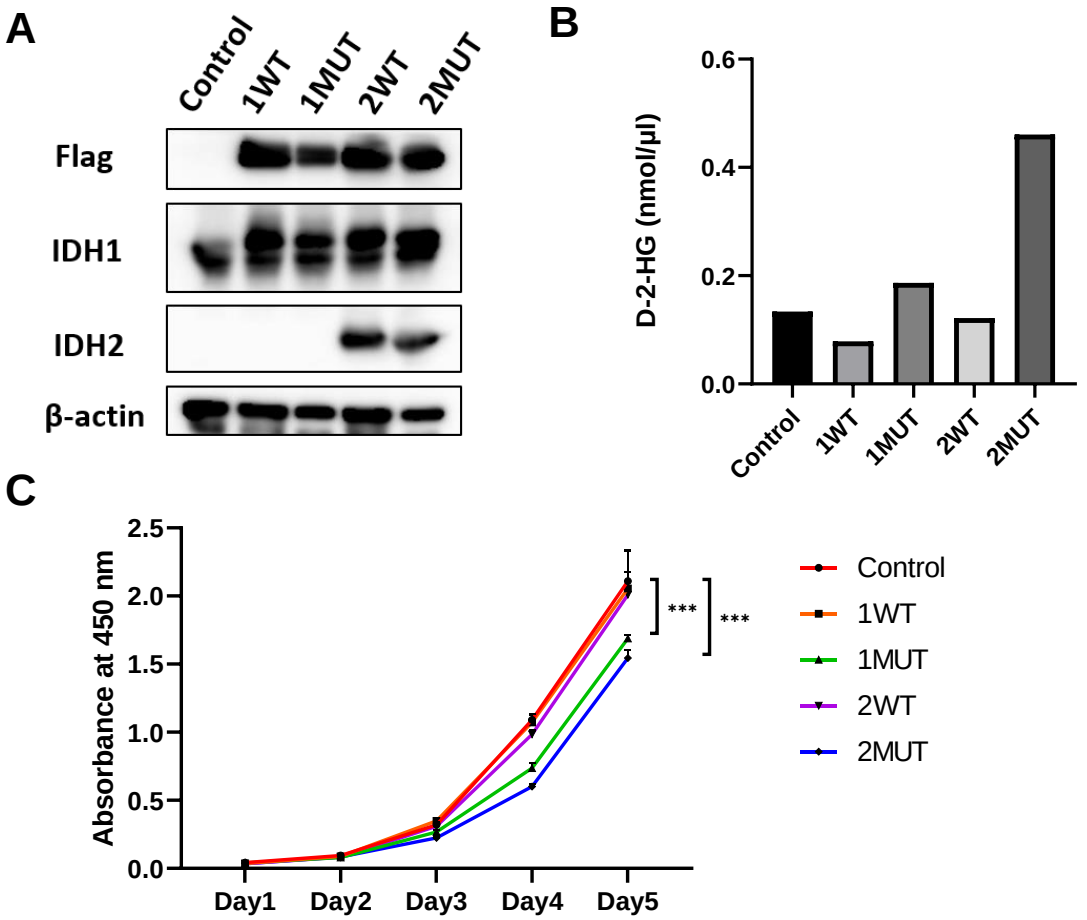

Figure 4. Effect of wild type and mutant IDH1/2 on 2-HG and cellular proliferation.
(A) Western blot analysis of the MEF cells stably expressing wild-type or mutant IDH1/2 (MEF-1WT, MEF-2WT, MEF-1MUT, and MEF-2MUT), and control MEF cells. Expression of β-actin served as an internal control. The anti-IDH1 antibody recognized not only endogenously and exogenously expressed IDH1 but also exogenously expressed IDH2. The anti-IDH2 antibody recognized both endogenous and exogenous expression of IDH2. Expression of endogenous IDH2 is too low to be detected in the MEF cells.
(B) Concentration of 2-HG in the lysates from cells indicated in (A). The data represents from three independent experiments.
(C) The proliferation of cells was measured by WST-8 assay. The data represents mean ± SD from triplicate experiments. *** $p < 0.001$.

Next, I analyzed the effect of these mutants on cell proliferation. The proliferation of the control cells, MEF-1WT, MEF-2WT, MEF-1MUT, and MEF-2MUT

were examined using a WST-8 assay. Unexpectedly, exogenous expression of the mutant IDH1 as well as the mutant IDH2 slightly suppressed the proliferation of MEF cells (MEF-1MUT and MEF-2MUT) compared to the control cells, MEF-1WT, or MEF-2WT (Figure 4C).

2. Identification of pathways and genes commonly regulated by cancer-associated IDH2 mutant and 2-HG

To clarify the effect of IDH2 mutant through accumulated 2-HG, I performed RNA-seq analysis. Comparison of expression profiles of the MEF cells expressing mutant IDH2 (2MUT) with control MEF cells (Control) identified a total of 575 up-regulated and 716 down-regulated genes (Figure 5A). I also compared expression profiles of MEF cells treated with 300 μM of membrane-permeant 2-HG with non-treated MEF cells, and found a total of 884 up-regulated genes and 1046 down-regulated genes by the 2-HG treatment. Combination of these data identified a total of 117 genes including 37 commonly up-regulated genes (Figure 5B-C) and 80 commonly down-regulated genes (Figure 5D-E) by the IDH2 mutant and 2-HG treatment.

A

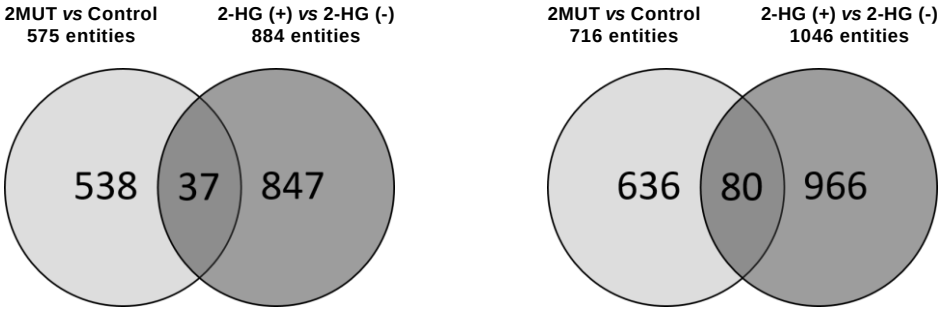
2MUT *vs* Control
575 entities
2-HG (+) *vs* 2-HG (-)
884 entities
538
37
847
2MUT *vs* Control
716 entities
2-HG (+) *vs* 2-HG (-)
1046 entities
636
80
966

B

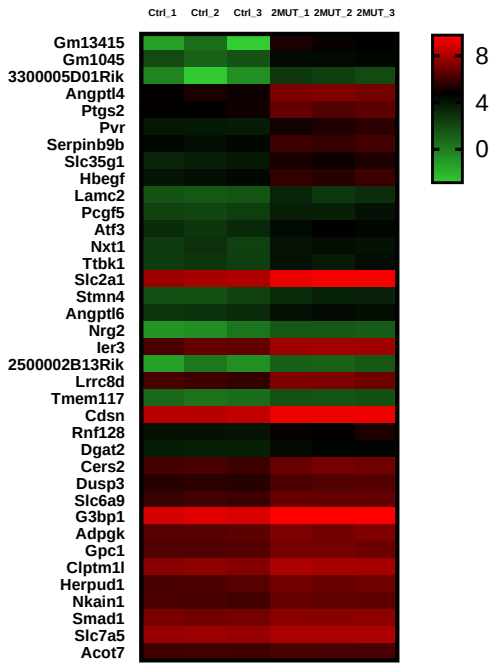
Ctrl_1
Ctrl_2
Ctrl_3
2MUT_1
2MUT_2
2MUT_3
Gm13415
Gm1045
3300005D01Rik
Angptl4
Ptgs2
Pvr
Serpinb9b
Slc35g1
Hbegf
Lamc2
Pcgf5
Atf3
Nxt1
Ttbk1
Slc2a1
Stmn4
Angptl6
Nrg2
Ier3
2500002B13Rik
Lrrc8d
Tmem117
Cdsn
Rnf128
Dgat2
Cers2
Dusp3
Slc6a9
G3bp1
Adpgk
Gpc1
Clptm1l
Herpud1
Nkain1
Smad1
Slc7a5
Acot7
8
4
0

C

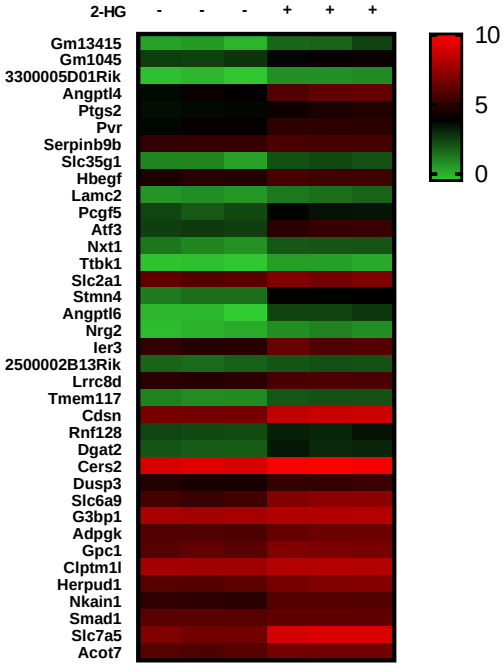
2-HG
- - - + + +
Gm13415
Gm1045
3300005D01Rik
Angptl4
Ptgs2
Pvr
Serpinb9b
Slc35g1
Hbegf
Lamc2
Pcgf5
Atf3
Nxt1
Ttbk1
Slc2a1
Stmn4
Angptl6
Nrg2
Ier3
2500002B13Rik
Lrrc8d
Tmem117
Cdsn
Rnf128
Dgat2
Cers2
Dusp3
Slc6a9
G3bp1
Adpgk
Gpc1
Clptm1l
Herpud1
Nkain1
Smad1
Slc7a5
Acot7
10
5
0

Figure 5. Genes with altered expression by the IDH2 mutant or 2-HG treatment.
(A) Venn diagram of up-regulated (left) and down-regulated (right) genes by the overexpression of the IDH2 mutant or the treatment with 2-HG in MEF cells.
(B-E) Heatmap of the 37 commonly up-regulated (B and C) and the 80 commonly down-regulated (D and E) genes by the IDH2 mutant and 2-HG.

I then carried out GSEA for the gene profiles altered by the mutant IDH2, and those altered by 2-HG (Figure 6 and 7; Table 5 and 6). GSEA showed enrichment of signatures corresponding to "PI3K/Akt/mTOR signaling", "glycolysis" and "reactive oxygen species" in both cells expressing the IDH2 mutant and treated with 2-HG. In addition, gene sets correlated with "HIF1 pathway" were enriched in the *IDH2* mutant cells but not in the cells with 2-HG treatment. On the other hand, genes associated with "VEGF pathway" were enriched by 2-HG treatment, but not in the *IDH2* mutant cells.

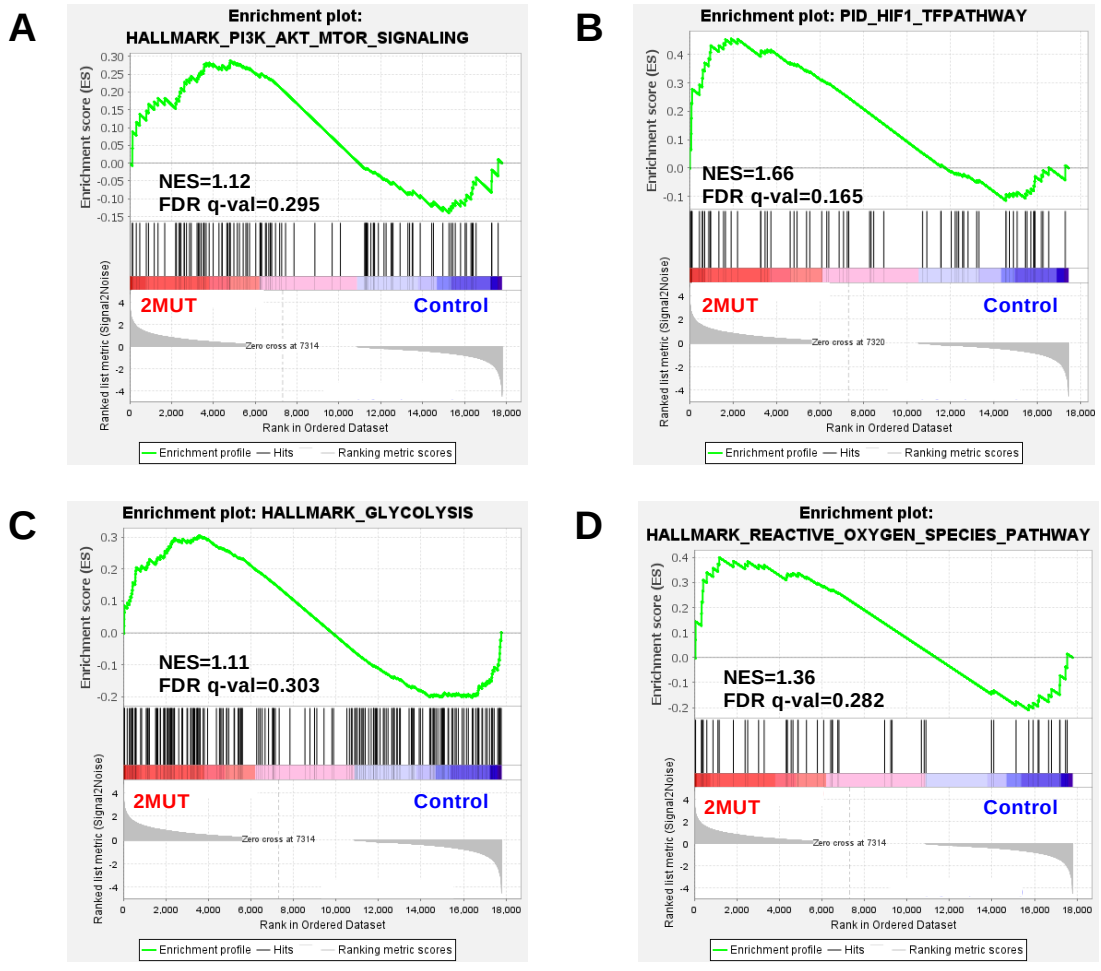

Figure 6. Four enriched signatures by the IDH2 mutant.
GSEA plot of enriched PI3K_AKT_MTOR signaling (A), PID_HIF1_TF pathway (B), glycolysis (C), and reactive oxygen species pathway (D) by the expression of the IDH2 mutant in MEF cells.

Table 5. Gene sets enriched in MEF-2MUT cells.

Name of gene set	NES	FDR q-value
HALLMARK_XENOBIOTIC_METABOLISM	1.43	0.284
HALLMARK_PANCREAS_BETA_CELLS	1.41	0.231
HALLMARK_REACTIVE_OXYGEN_SPECIES_ PATHWAY	1.36	0.282
HALLMARK_TNFA_SIGNALING_VIA_NFKB	1.36	0.252
HALLMARK_TGF_BETA_SIGNALING	1.35	0.211
HALLMARK_ADIPOGENESIS	1.33	0.221
HALLMARK_ESTROGEN_RESPONSE_EARLY	1.26	0.273
HALLMARK_COAGULATION	1.25	0.245
HALLMARK_INFLAMMATORY_RESPONSE	1.24	0.227
HALLMARK_PROTEIN_SECRETION	1.23	0.209
HALLMARK_P53_PATHWAY	1.22	0.219
HALLMARK_UNFOLDED_PROTEIN_RESPONSE	1.21	0.242
HALLMARK_CHOLESTEROL_HOMEOSTASIS	1.20	0.235
HALLMARK_HYPOXIA	1.18	0.268
HALLMARK_MYOGENESIS	1.17	0.271
HALLMARK_UV_RESPONSE_DN	1.14	0.300
HALLMARK_ALLOGRAFT_REJECTION	1.13	0.293
HALLMARK_PI3K_AKT_MTOR_SIGNALING	1.12	0.295
HALLMARK_GLYCOLYSIS	1.11	0.303
HALLMARK_BILE_ACID_METABOLISM	1.10	0.301

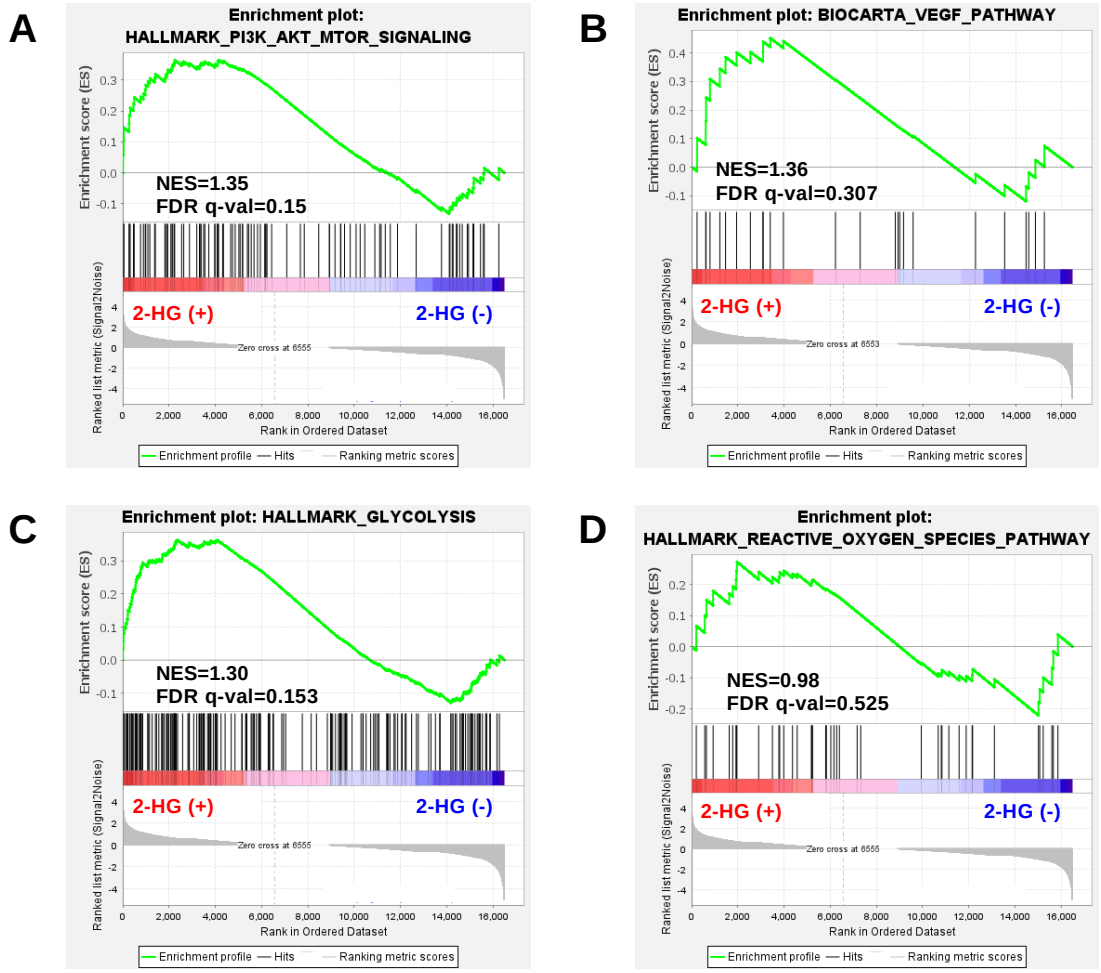

Figure 7. Four enriched signatures by 2-HG treatment in MEF cells.
GSEA plots of enriched PI3K_AKT_MTOR signaling (A), VEGF pathway (B), glycolysis (C), and reactive oxygen species pathway (D) by the treatment with 2-HG in MEF cells.

Table 6. Gene sets enriched in 2HG treated MEF.

Name of gene set	NES	FDR q-value
HALLMARK_MITOTIC_SPINDLE	1.64	0.054
HALLMARK_UNFOLDED_PROTEIN_RESPONSE	1.53	0.078
HALLMARK_G2M_CHECKPOINT	1.51	0.088
HALLMARK_MTORC1_SIGNALING	1.46	0.100
HALLMARK_DNA_REPAIR	1.40	0.119
HALLMARK_PI3K_AKT_MTOR_SIGNALING	1.35	0.150
HALLMARK_E2F_TARGETS	1.34	0.139
HALLMARK_MYC_TARGETS_V2	1.32	0.142
HALLMARK_GLYCOLYSIS	1.30	0.153
HALLMARK_MYC_TARGETS_V1	1.29	0.151
HALLMARK_OXIDATIVE_PHOSPHORYLATION	1.20	0.200
HALLMARK_SPERMATOGENESIS	1.11	0.284
HALLMARK_REACTIVE_OXYGEN_SPECIES_ PATHWAY	0.98	0.525
HALLMARK_HYPOXIA	0.96	0.541
HALLMARK_FATTY_ACID_METABOLISM	0.77	0.890

Next, to understand the biological alterations by the *IDH2* mutation through 2-HG accumulation, I performed KEGG pathway analysis with the 117 overlapped genes using curated gene sets in the MSigDB. I found significant enrichment of genes associated with “ECM-receptor interaction”, “focal adhesion”, “TGF-beta signaling pathway”, “pathways in cancer”, “cytosolic DNA-sensing pathway”, and “cell adhesion molecules” (Figure 8, Table 7). These data suggest that accumulated 2-HG may alter communication between cells and matrix, cellular adhesion, and signal transduction pathways, and that these biological alterations may play a role in human carcinogenesis.

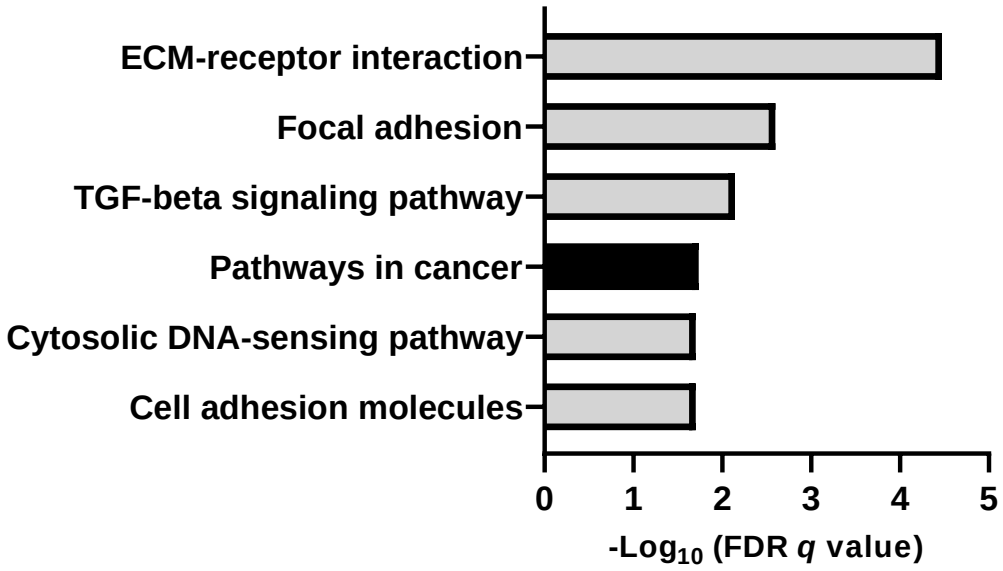

Figure 8. FDRs of enriched gene sets by the IDH2 mutant and 2-HG treatment. FDRs of six gene sets identified by KEGG pathway analysis.

Table 7. Details of KEGG pathway analysis by MSigDB.

Name of Gene Set	Description	Overlapped gene symbols	p-value	FDR q-value
KEGG_ECM_RECEPTOR_ INTERACTION	ECM-receptor interaction	*Lamc2*, *Thbs2*, *Col1a2*, *Col3a1*, *Col11a1*, *Sdc2*	1.82E-07	3.38E-05
KEGG_FOCAL_ ADHESION	Focal adhesion	*Lamc2*, *Thbs2*, *Col1a2*, *Col3a1*, *Col11a1*, *Cav1*	2.72E-05	2.53E-03
KEGG_TGF_BETA_ SIGNALING_PATHWAY	TGF-beta signaling pathway	*Thbs2*, *Bmp4*, *Dcn*, *Smad1*	1.16E-04	7.17E-03
KEGG_PATHWAYS_ IN_CANCER	Pathways in cancer	*Lamc2*, *Bmp4*, *Slc2a1*, *Ptgs2*, *Mmp9*, *Jup*	3.96E-04	1.84E-02
KEGG_CYTOSOLIC_DNA_ SENSING_PATHWAY	Cytosolic DNA-sensing pathway	*Ccl5*, *Sting1*, *Zbp1*	5.67E-04	1.98E-02
KEGG_CELL_ADHESION_ MOLECULES_CAMS	Cell adhesion molecules (CAMs)	*Sdc2*, *Hla-a*, *Nlgn2*, *Pvr*	6.39E-04	1.98E-02

3. Identification of Glut1 as a target molecule induced by the IDH1/2 mutants and 2-HG

To identify genes involved in *IDH1/2* mutation-associated carcinogenesis, I searched genes commonly altered by the IDH2 mutant and the treatment with 2-HG. In the six enriched gene sets detected by KEGG pathway analysis, I focused on the six genes in "pathways in cancer" (Table 7). The six genes included three, *Ptgs2*, *Lamc2* and *Slc2a1*, which were upregulated, and three, *Bmp4*, *Mmp9* and *Jup*, which were down-regulated (Table 7). Quantitative RT-PCR analysis confirmed that expression of *Ptgs2*, *Lamc2*, and *Slc2a1* were elevated by the IDH2 mutant (Figure 9A-C) and 2-HG treatment (Figure 9D-F). Additionally, the expression levels of these genes were similarly enhanced by the IDH1 mutant (Figure 9A-C). These results suggested that the three genes may serve for molecular markers of the tumors with mutant IDH1/2 and/or elevated 2-HG.

Since *Slc2a1* encodes glucose transporter 1 (Glut1), a key molecule involved in cellular energy metabolism, I focused on this molecule in this study. Western blot analysis further corroborated increased expression of Glut1 by the IDH mutants (Figure 9G) and the treatment with 2-HG in MEF cells (Figure 9H).

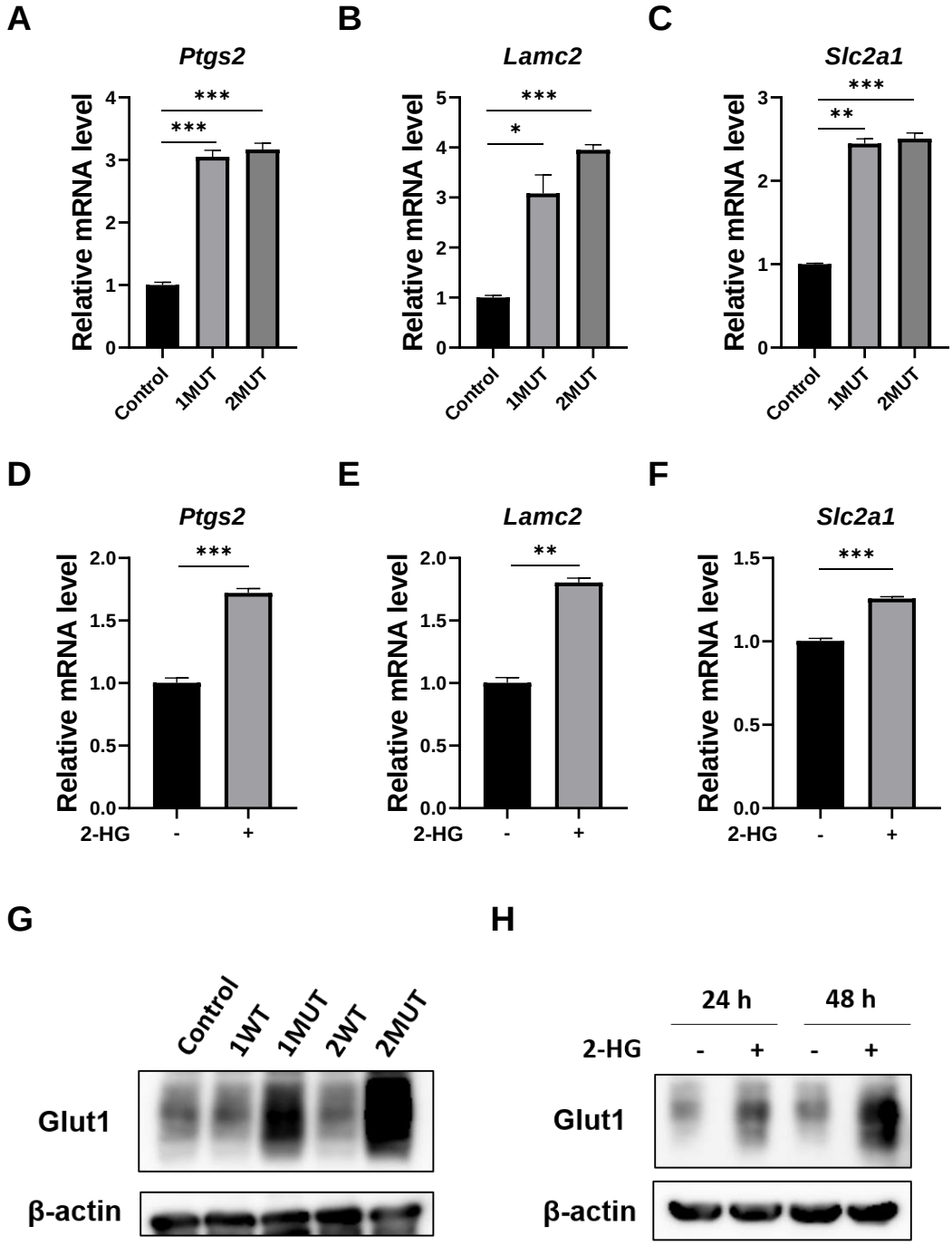

Figure 9. Enhanced expression of Glut1 by the expression of IDH1/2 mutants and 2-HG.

(A-C) Induction of *Ptgs2* (A), *Lamc2* (B), and *Slc2a1* (C) in MEF cells stably expressing the IDH1 or IDH2 mutant. Expression was determined by real time-PCR. Expression of *Gapdh* was used as an internal control. The data represents mean ± SD from triplicate experiments. * $p < 0.05$, ** $p < 0.01$, *** $p < 0.001$.

(D-F) Induction of *Ptgs2* (D), *Lamc2* (E), and *Slc2a1* (F) in MEF cells treated with 300 μM of 2-HG for 24 h. ** $p < 0.01$, *** $p < 0.001$.

(G) Elevated expression of Glut1 protein by the IDH1/2 mutants**.** Expression of β-actin served as an internal control. The data represents from three independent experiments.
(H) Elevated expression of Glut1 protein in response to the treatment with 300 μM of 2-HG. Cell lysates were harvested at 24 h or 48 h after treatment and subjected for western blotting.

4. Enhanced glucose uptake and glycolysis by the IDH1/2 mutants

Since Glut1, a glucose transporter that facilitate glycolysis, was up-regulated by the IDH1/2 mutants at least in part through the increase of 2-HG, I investigated the glucose uptake in MEF-1WT, MEF-1MUT, MEF-2WT, MEF-2MUT and the control cells, using an enzymatic assay. As I expected, the capacity of glucose uptake in the MEF cells (MEF-1MUT and MEF-2MUT) were significantly enhanced by the IDH1/2 mutants (Figure 10A).

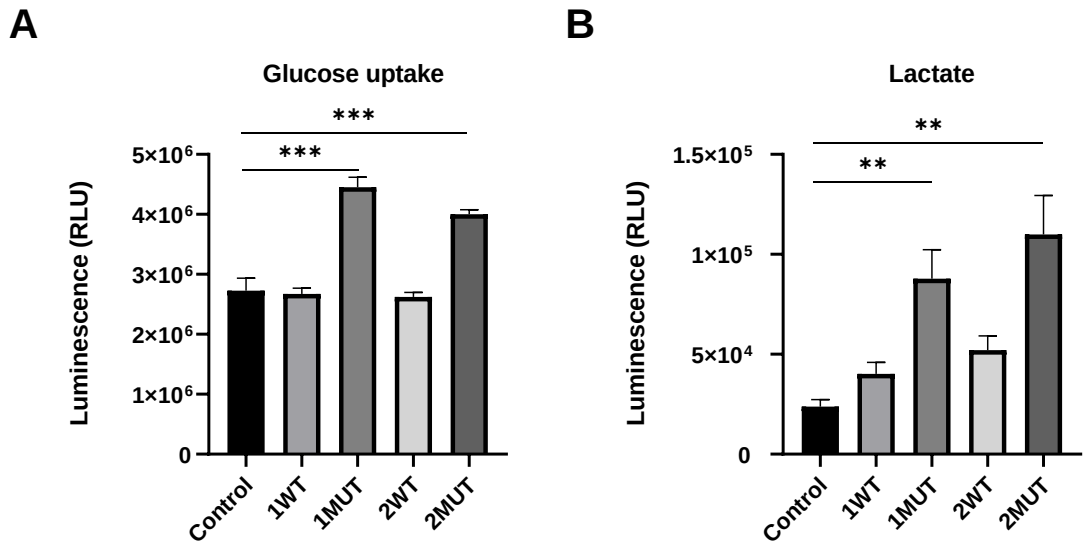

Figure 10. Augmentation of glucose uptake and intracellular lactate levels by the IDH1/2 mutants.
(A) Glucose uptake levels in MEF-1WT, MEF-1MUT, MEF-2WT, MEF-2MUT, and the control cells were measured by a bioluminescent assay based on the detection of 2DG6P. The data represents mean ± SD from triplicate experiments. *** $p < 0.001$.
(B) Intracellular lactate levels in the MEF cells indicated in (A) were measured by a bioluminescent assay for the detection of L-lactate. The data represents mean ± SD from triplicate experiments. ** $p < 0.01$.

I further measured possible alteration of intracellular lactate, the end product of

glycolysis. In concert with the elevated expression of Glut1, an increase of intracellular lactate level was observed in MEF-1MUT and MEF-2MUT, suggesting that the up-regulation of Glut1 by IDH1/2 mutants contributes to the induction of glycolysis in MEF cells (Figure 10B).

5. Involvement of PI3K/Akt/mTOR pathway in the regulation of Glut1 induction by cancer-associated *IDH1/2* mutations

It was reported that *IDH1/2* mutations activate the PI3K/Akt/mTOR pathway[66]. Consistently, the GSEA analyses identified the association of the *IDH2* mutation with PI3K/Akt/mTOR signaling (Figure 6A). Thus, I investigated phosphorylation of Akt and ribosomal protein S6 kinase (S6k) in MEF-1WT, MEF-1MUT, MEF-2WT, and MEF-2MUT cells. As a result, expression of phosphorylated S6k and Akt on Ser473 were increased in MEF-1MUT and MEF-2MUT cells (Figure 11A), indicating both mTORC1 and mTORC2 were activated. In addition, the IDH1/2 mutants also induced elevated phosphorylation of Akt on Thr308 (Figure 11A), which is regulated by PDK1. These data indicate activation of the PI3K/PDK1/Akt/mTOR cascade by the *IDH1/2* mutations. I further studied whether the induced Glut1 expression by the *IDH1/2* mutations is regulated through the activation of PI3K/Akt/mTORC1 pathway. As shown in Figure 11B, knockdown of *Akt1*, *Akt2* and *Akt3* by siRNA decreased Glut1 expression in the MEF cells with the IDH1/2 mutants. In addition, treatment with PI-103, a multi-targeted PI3K inhibitor, and rapamycin, an inhibitor of mTORC1, markedly reduced Glut1 expression (Figure 11C, 11D), suggesting that PI3K/Akt/mTORC1 pathway is involved in the increased Glut1 expression by the IDH mutants.

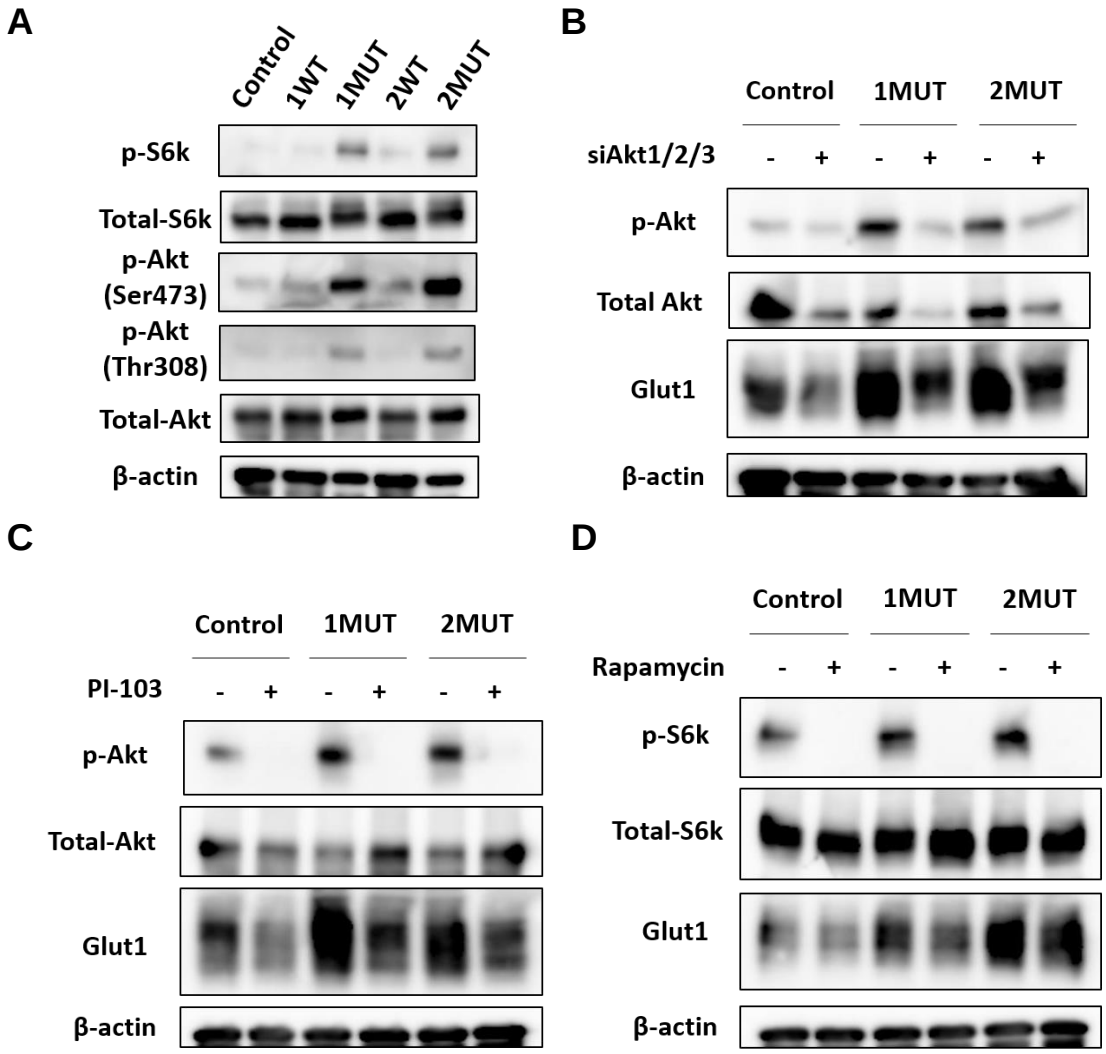

Figure 11. Involvement of the PI3K/Akt/mTOR pathway in the enhancement of Glut1 by the IDH1/2 mutants.

(A) Phosphorylation of S6k and Akt in MEF-1WT, MEF-1MUT, MEF-2WT, MEF-2MUT, and the control cells. Expression of β-actin served as an internal control.

(B) Involvement of Akts in the induction of Glut1. Akt1/2/3 were silenced with a mixture of *Akt1*, *Akt2* and *Akt3* (Akt1/2/3) siRNA for 48 h.

(C and D) MEF-1MUT, MEF-2MUT and control cells were treated with 1 μM of PI-103 (C) or 20 nM of rapamycin (D) for 24 h. Lysate with/without the treatment were subjected for western blotting.

6. Involvement of Hif1α in the regulation of Glut1 by the *IDH1/2* mutations

Reportedly, GLUT1 expression is augmented under hypoxia through the induction of HIF1α in cancer cells[56]. The GSEA analyses in current study also showed that genes correlated with the "HIF1 pathway" were enriched in MEF-2MUT (Figure 6B). Therefore, I investigated whether the IDH1/2 mutants enhance the expression of Hif1α. Western blot analysis showed that exogenous expression of the IDH1 or IDH2 mutant increased the expression levels of Hif1α, and that knockdown of Hif1α reduced Glut1 expression in MEF-1MUT and MEF-2MUT cells (Figure 12A). To investigate the association between PI3K/Akt/mTORC1 pathway and Hif1Iα expression in *IDH1/2* mutant cells, I treated MEF-1MUT, MEF-2MUT, and control cells with rapamycin. As a result, qPCR analysis revealed that treatment of rapamycin reduced Hif1α expression by 25%, 36%, and 30%, in control, MEF-1MUT, and MEF-2MUT cells, respectively (Figure 12B). It is of note that rapamycin markedly decreased the Hif1α protein in these cells (Figure 12C), suggesting that post-transcriptional regulation plays a major role in expression of Hif1α. These results indicate that the PI3K/Akt/mTORC1-Hif1α axis is involved in the induction of Glut1 by the IDH1/2 mutants.

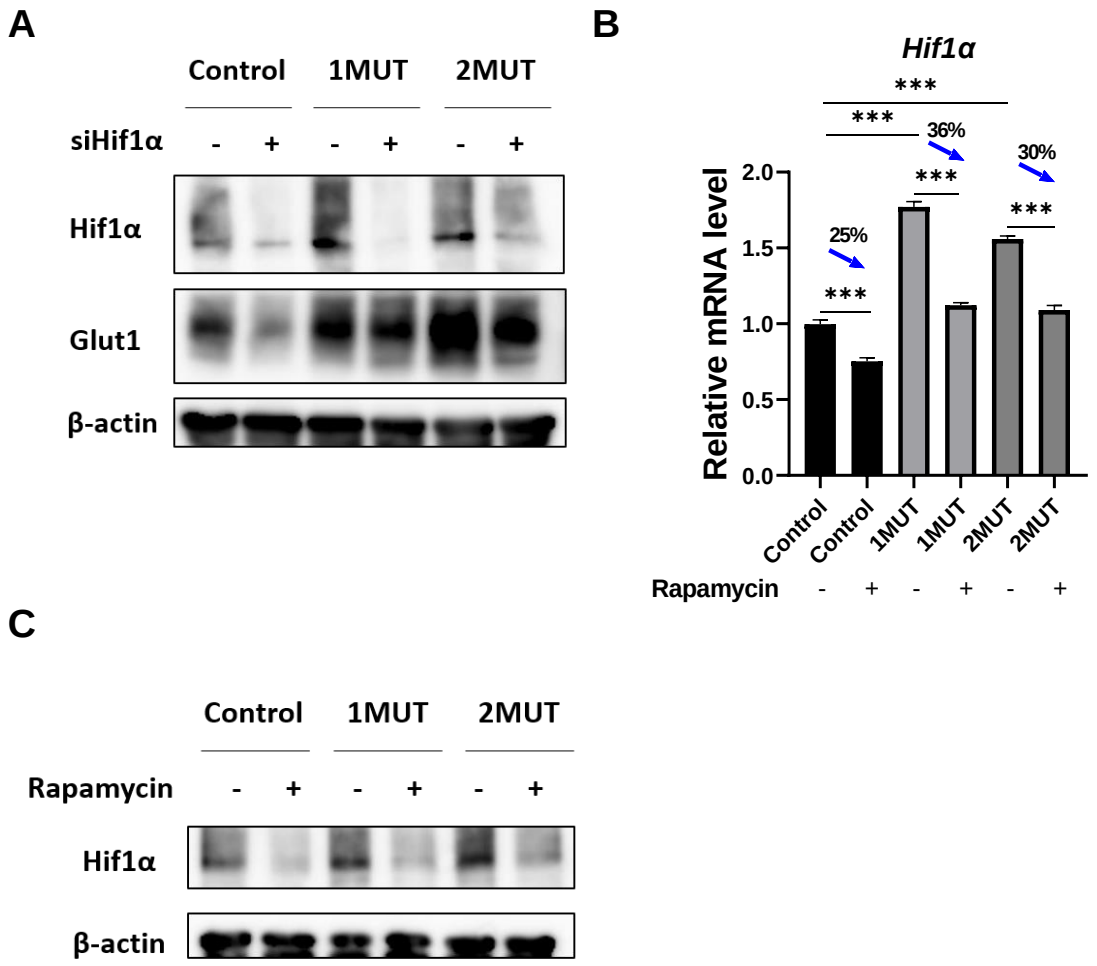

Figure 12. Involvement of Hif1α in the induction of Glut1 in MEF cells.

(A) MEF-1MUT, MEF-2MUT, and the control cells were treated with *Hif1α* or control siRNA for 48 h. Expression of β-actin served as an internal control.

(B) MEF-1MUT, MEF-2MUT, and control cells were treated with 20 nM of rapamycin for 24 h. Expression was determined by real time-PCR. Expression of *Gapdh* was used as an internal control. The data represent mean ± SD from triplicate experiments. *** p ＜0.001.

(C) The lysates of MEF cells indicated in (B) were subjected for western blotting.

7. Involvement of the *IDH1/2* mutations in murine liver tumorigenesis

To investigate the effect of *IDH1*^{R132C} and *IDH2*^{R172S} mutants in liver carcinogenesis, I generated liver-specific *IDH1/2* mutation knockin mice (Figure 13). Conditional knockin mice carrying *IDH1*^{R132C} or *IDH2*^{R172S} with a LoxP-STOP-LoxP (LSL) cassette preceding each gene were crossed with *Alb-Cre* mice expressing Cre recombinase in the liver.

Since liver-specific *IDH1/2* mutation knockin mice (*Alb-cre; LSL-IDH1*^{R132C} and *Alb-cre; LSL-IDH2*^{R172S}) did not develop hepatic tumors, I introduced an oncogenic *Kras* mutation in the knockin mice to investigate the role of *IDH1*^{R132C} and *IDH2*^{R172S} mutations in liver carcinogenesis. Mice carrying the conditional knockin allele of the *Kras*^{G12D} mutation (*LSL-Kras*^{G12D}) were then crossed with liver-specific *IDH1/2* mutation knockin mice to generate *Alb-cre; LSL-Kras*^{G12D} (*AK*)*; LSL-IDH1*^{R132C} (*AKIDH1*^{mut}) and *Alb-cre; LSL-Kras*^{G12D}*; LSL-IDH2*^{R172S} (*AKIDH2*^{mut}) mice (Figure 13).

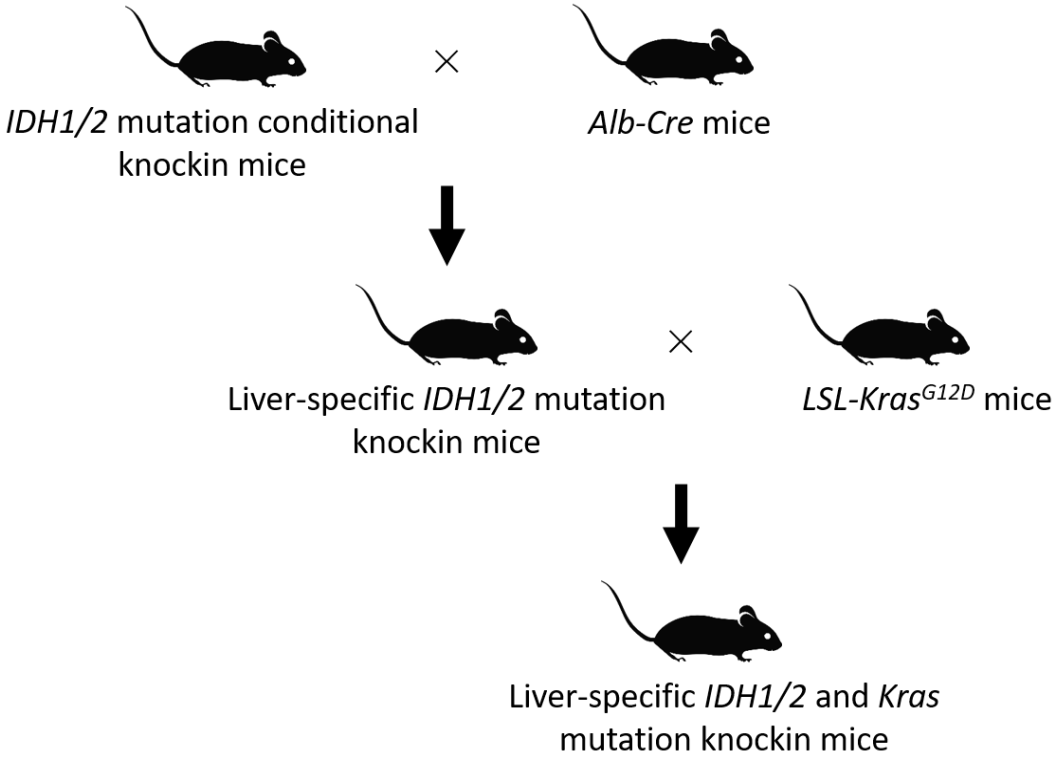

Figure 13. Strategy of generating liver-specific *IDH1/2* and *Kras* mutation double-knockin mice.
IDH1/2 mutation conditional knockin mice were crossed with *Alb-Cre* and *LSL-Kras*^{G12D} mice to generate mice with liver-specific IDH*1/2* and *Kras* mutations.

Analysis of survival of *AKIDH1*^{mut} and *AKIDH2*^{mut} mice showed that both *AKIDH1*^{mut} and *AKIDH2*^{mut} mice exhibited significantly shorter survival time compared with *AK* mice (Figure 14A). The median survival time of *AKIDH1*^{mut}, *AKIDH2*^{mut}, and *AK* mice was 259, 273, and 391 days, respectively. The majority of *AKIDH1*^{mut} and *AKIDH2*^{mut} mice showed apparent growth retardation compared with *AK* mice. Importantly, most of *AKIDH1*^{mut} and *AKIDH2*^{mut} mice showed abdominal distension within 11 months of age. Autopsies revealed enlargement of their liver due to the development of multiple hepatic tumors.

The ratios of liver weight to body weight were significantly increased in *AKIDH1*^{mut} and *AKIDH2*^{mut} mice compared with those in *AK* mice at the age of 11-13 months (Figure 14B). Although the average number of small tumors (within 5 mm in diameter) did not show significant difference among *AKIDH1*^{mut}, *AKIDH2*^{mut}, and *AK* mice, that of large hepatic tumors (over 5 mm in diameter) was significantly augmented in *AKIDH1*^{mut} and *AKIDH2*^{mut} mice compared with *AK* mice (Figure 14C, 14D).

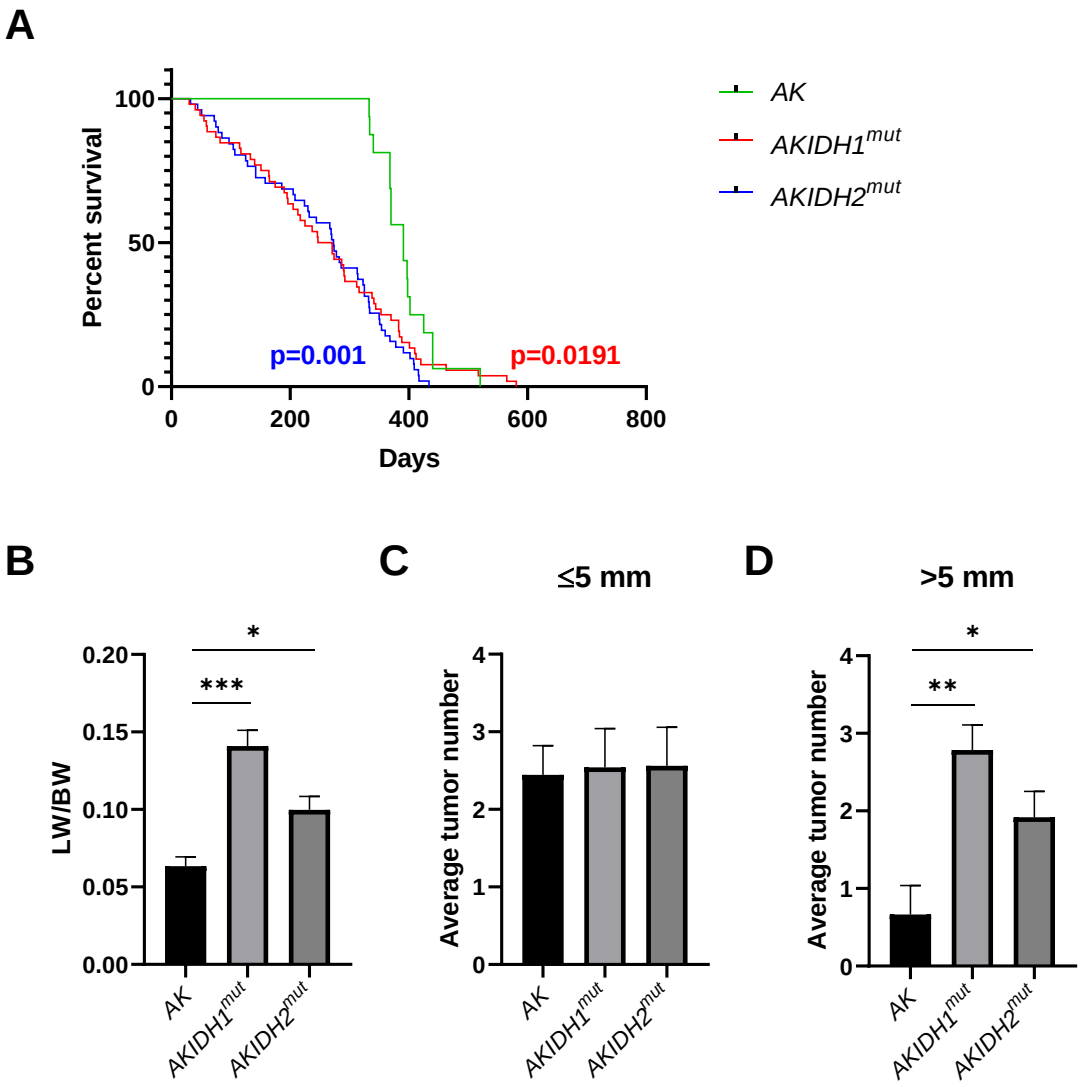

Figure 14. Survival and liver tumor burden in liver-specific *IDH1/2* and *Kras* mutations knockin mice.

(A) Survival curve of *Alb-cre; LSL-Kras^{G12D}; LSL-IDH1^{R132C}* (*AKIDH1^{mut}*) (n=52), *Alb-cre; LSL-Kras^{G12D}; LSL-IDH2^{R172S}* (*AKIDH2^{mut}*) (n=51) and *Alb-cre; LSL-Kras^{G12D}* (*AK*) (n=16) mice.

(B) Ratio of liver weight to body weight in *AKIDH1^{mut}* (n=45), *AKIDH2^{mut}* (n=39) and *AK* (n=12) mice. All mice were dissected at age of 12 ± 1 months. Data are presented as mean ± SD. * $p < 0.05$, *** $p < 0.001$.

(C and D) Average number of tumors, of which the diameters were less than or equal to 5 mm (C) or greater than 5 mm (D). The number of tumors developed per mouse indicated in (B) were counted macroscopically. Data are presented as mean ± SEM. * $p < 0.05$, ** $p < 0.01$.

Histological analysis of the hepatic tumors in *AK* mice (Figure 15) revealed that the multiple tumors resembled to hepatocellular carcinoma (HCC) or dysplastic nodule (DN), a precursor lesion of HCC, in agreement with a previous report[67], but no ICC-like tumors were observed in the liver of *AK* mice (Table 8). In contrast, *AKIDH1*^{mut} and *AKIDH2*^{mut} mice developed not only HCC or DN-like tumors but also ICC-like tumors that accompanied by a dense desmoplastic stroma surrounding the malignant ducts and gland. Additional immunohistochemical staining demonstrated positive-staining of Ck-19 in the ICC-like tumor cells (Figure 16), indicating cholangiocyte differentiation of the tumorous cells. In addition, the number of HCC/DN developed in *AKIDH1*^{mut} mice was greater than that in *AK* mice (Table 8). Although the incidence of HCC/DN in *AKIDH2*^{mut} mice was less than that in *AKIDH1*^{mut} or *AK* mice, the incidence of ICC in *AKIDH2*^{mut} mice was higher by 5.6-fold than that in *AKIDH1*^{mut} mice.

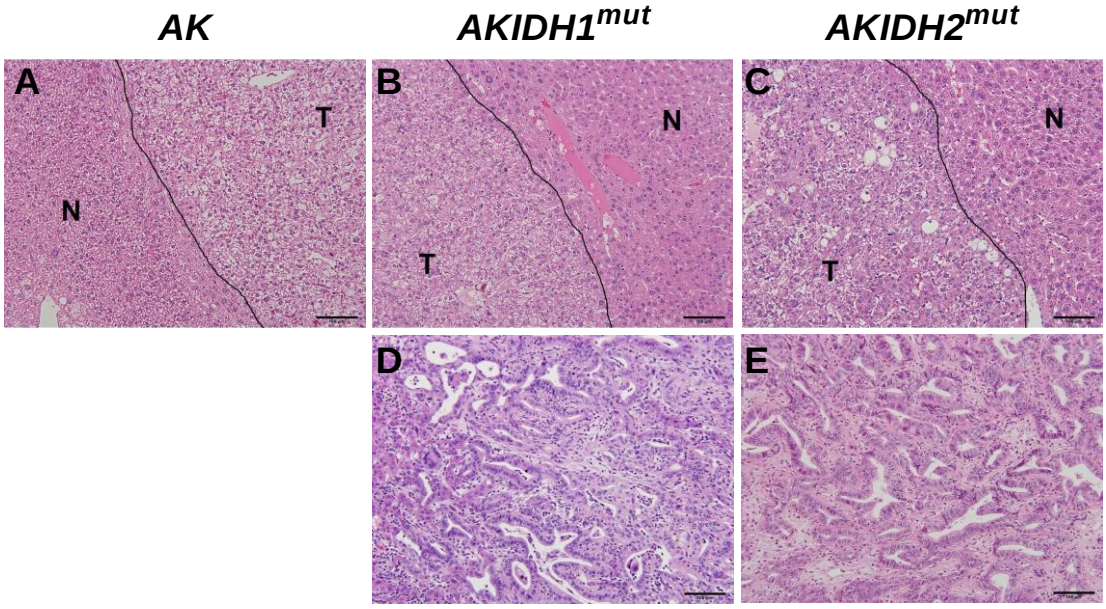

Figure 15. Histological analysis of the liver tissues in *AK*, *AKIDH1*^{mut}, and *AKIDH2*^{mut} mice.
(A-C) Representative images of hematoxylin and eosin (H&E) staining of non-tumorous

liver tissues (N) and HCC tissues (T) in *AK* (A), *AKIDH1*^{mut} (B), and *AKIDH2*^{mut} (C) mice. Bar, 100 μm. Line showed the boundary between tumorous and non-tumorous area.
(D and E) Representative images of H&E staining of the ICC tissues in *AKIDH1*^{mut} (D) and *AKIDH2*^{mut} (E) mice. Bar, 100 μm.

Table 8. Tumor incidence in the liver of *AK*, *AKIDH1*^{mut}, and *AKIDH2*^{mut} mice.

	AK	***AKIDH1*^{mut}**	***AKIDH2*^{mut}**
ICC* (Male/Female)	0	5 (2/3)	23 (11/12)
HCC/DN (Male/Female)	9 (6/3)	55 (35/20)	21 (13/8)
No tumor**	8	14	16
Total	17	74	60
ICC incidence	0	6.8%	38.3%
HCC/DN incidence	52.9%	74.3%	35%

* Including mixed type, ** Including tumor size ≤ 1 mm or number of tumor ≤ 5.

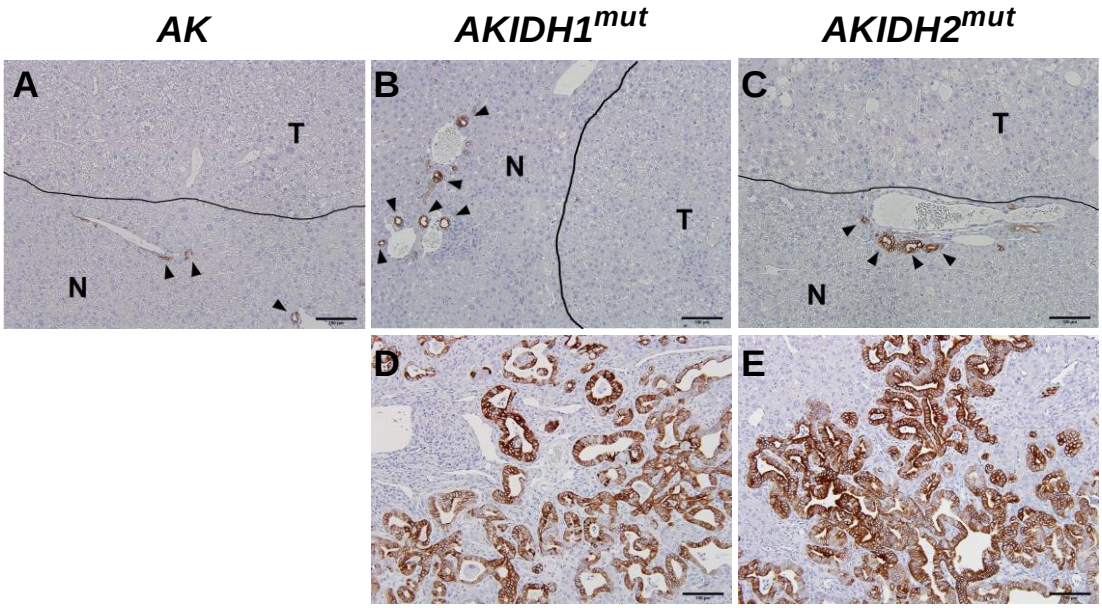

Figure 16. Expression of Ck19 in *AK*, *AKIDH1*^{mut}, and *AKIDH2*^{mut} mice.
(A-C) Immunohistochemical staining of Ck19 in non-tumorous liver tissues (N) and HCC tissues (T) of *AK* (A), *AKIDH1*^{mut} (B) and *AKIDH2*^{mut} (C) mice. Bar, 100 μm. Line showed the boundary between tumorous and non-tumorous area. Arrow indicated

interlobular bile ducts.
(D and E) Immunohistochemical staining of Ck19 in ICC tissues of *AKIDH1*^{mut} (D) and *AKIDH2*^{mut} (E) mice. Bar, 100 μm.

To confirm the recombination of the LSL cassette in *AKIDH1*^{mut} and *AKIDH2*^{mut} mice, I performed IHC of GFP, because the Cre-mediated recombination results in the expression of EGFP in the conditional *IDH1/2* mutation alleles (Figure 3). Compared with *AK* mice, GFP expression was detected in hepatocytes, intrahepatic bile ducts, and liver tumors, but not in stromal tissues in the liver of *AKIDH1*^{mut} or *AKIDH2*^{mut} mice (Figure 17). These results confirmed the precise expression of IDH1/2 mutants in the liver of these mouse models. Furthermore, immunohistological staining illustrated strong Ki-67 staining in both HCC/DN-like and ICC-like tumorous cells compared with non-tumorous hepatocytes in *AK*, *AKIDH1*^{mut}, and *AKIDH2*^{mut} mice (Figure 18), suggesting enhanced proliferation of the tumorous cells.

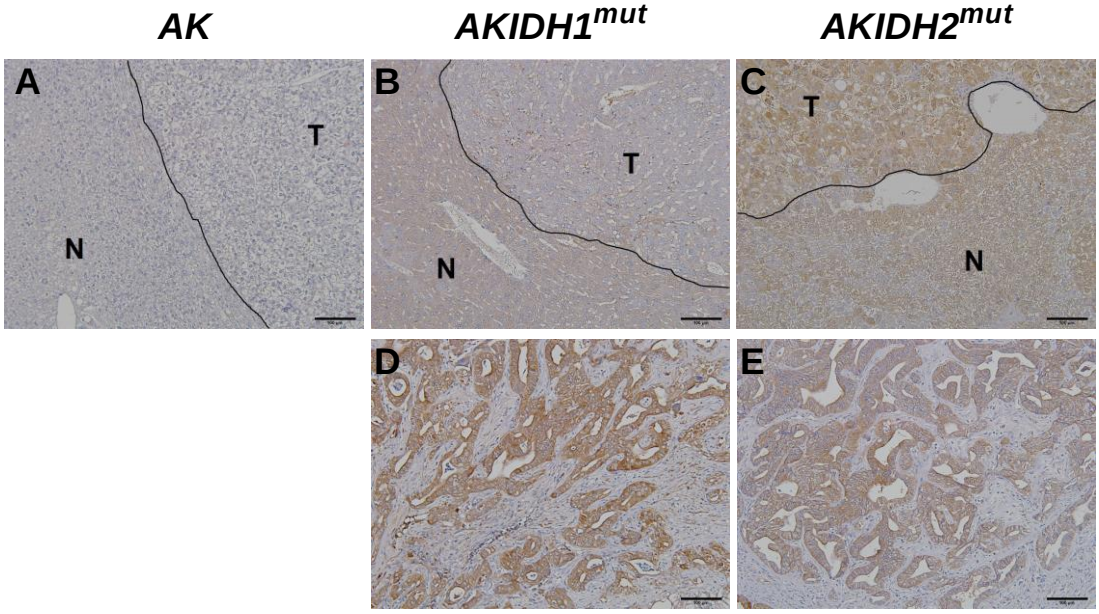

Figure 17. Expression of GFP, a surrogate marker for expression of IDH1/2 mutants, in *AK*, *AKIDH1*^{mut}, and *AKIDH2*^{mut} mice.
(A-C) Immunohistochemical staining of GFP in non-tumorous liver tissues (N) and HCC

tissues (T) of *AK* (A), *AKIDH1*^{mut} (B) and *AKIDH2*^{mut} (C) mice. Bar, 100 μm. Line showed the boundary between tumorous and non-tumorous area.
(D and E) Immunohistochemical staining of GFP in ICC tissues of *AKIDH1*^{mut} (D) and *AKIDH2*^{mut} (E) mice. Bar, 100 μm.

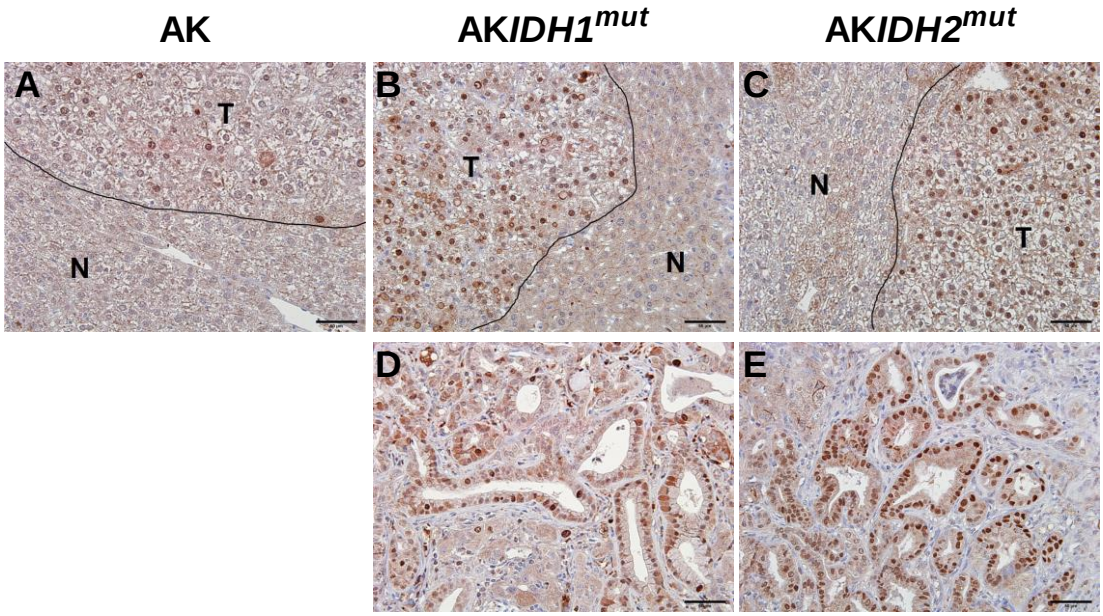

Figure 18. Expression of Ki-67 in *AK*, *AKIDH1*^{mut}, and *AKIDH2*^{mut} mice.
(A-C) Immunohistochemical staining of Ki-67 in non-tumorous liver tissues (N) and HCC tissues (T) of *AK* (A), *AKIDH1*^{mut} (B) and *AKIDH2*^{mut} (C) mice. Bar, 50 μm. Line showed the boundary between tumorous and non-tumorous area.
(D and E) Immunohistochemical staining of Ki-67 in ICC tissues of *AKIDH1*^{mut} (D) and *AKIDH2*^{mut} (E) mice. Bar, 50 μm.

Collectively, these data demonstrated that both *IDH1* and *IDH2* mutations identified in human cancer play a vital role in murine liver carcinogenesis. In addition, *IDH2*^{R172S} mutation may exert stronger effect on the development of ICC than *IDH1*^{R132C} mutation in the context of oncogenic *Kras*-induced murine liver tumorigenesis.

8. Enhanced expression of Glut1 by the IDH1/2 mutants in murine liver

To verify the *in vitro* findings of enhanced Glut1 expression by IDH1 and IDH2 mutants *in vivo*, I analyzed the expression of Glut1 in the liver of *AK*, *AKIDH1*^{mut} and *AKIDH2*^{mut} mice. As shown in Figure 19, immunohistochemical staining with an anti-Glut1 antibody showed an endogenous expression of Glut1 protein located on cell membranes. Enhanced positive staining was detected in the liver tissue of *AKIDH1*^{mut} and *AKIDH2*^{mut} mice compared with *AK* mice, especially in interlobular bile ducts. Expression of Glut1 was elevated in HCC compared with adjacent non-tumorous liver tissues (Figure 19E and F). Furthermore, ICC-like tumors in the liver of *AKIDH1*^{mut} and *AKIDH2*^{mut} mice was more strongly stained with anti-Glut1 antibody than non-tumorous tissues (Figure 19G and H). Real-time PCR analysis of the tumorous (HCC/DN and ICC) and non-tumorous tissues in *AKIDH1*^{mut} and *AKIDH2*^{mut} mice exhibited increased *Slc2a1* mRNA in the tumorous tissues compared to non-tumorous tissues (Figure 19I and J). These data corroborated augmented Glut1 expression by the IDH1/2 mutants in the murine liver, and suggested that enhanced Glut1 expression might be associated with the hepatic carcinogenesis.

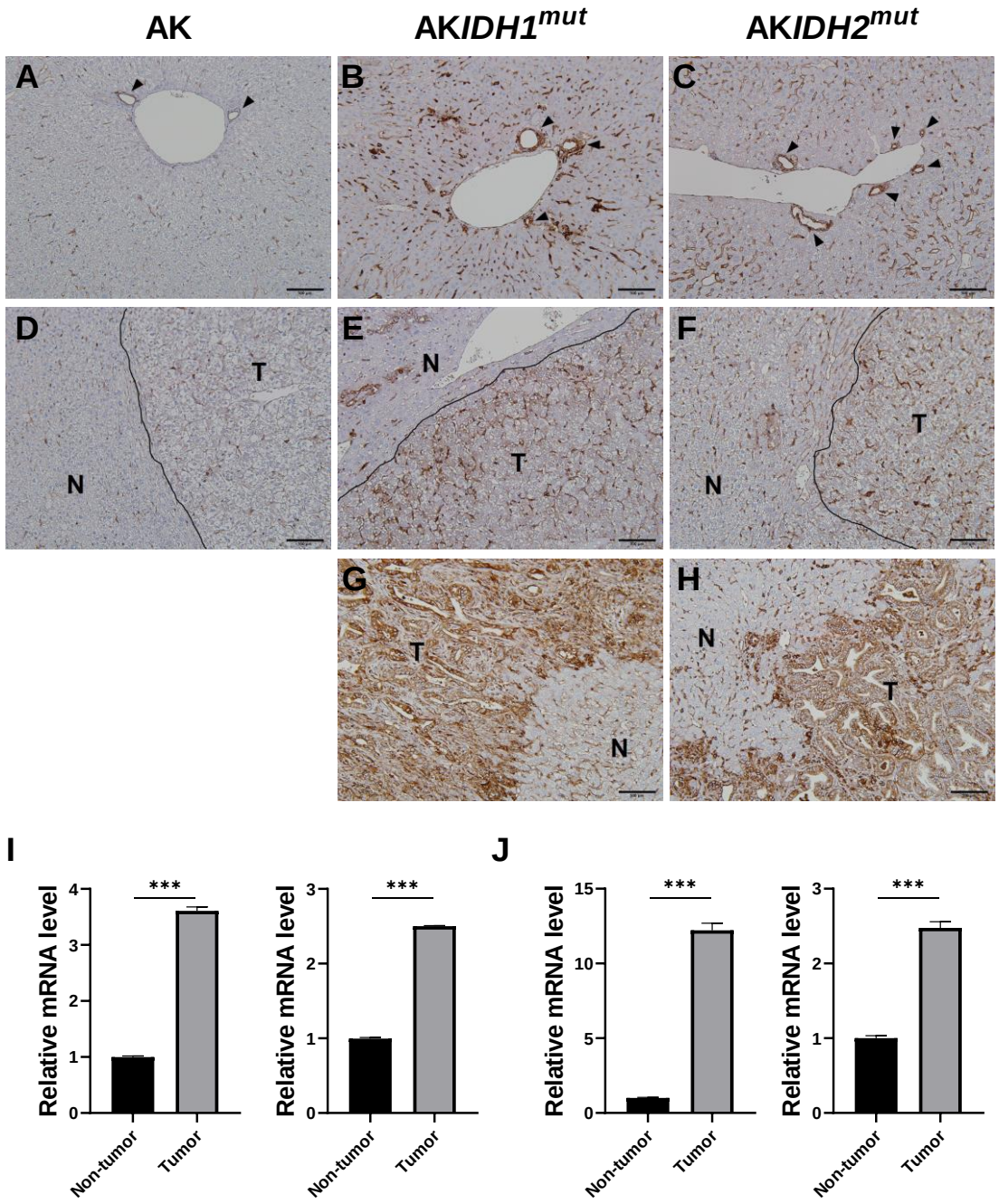

Figure 19. Expression of Glut1 in AK, AKIDH1^{mut}, and AKIDH2^{mut} mice.

(A-C) Immunohistochemical staining of Glut1 in interlobular bile ducts in *AK* (A), *AKIDH1^{mut}* (B) and *AKIDH2^{mut}* (C) mice. Bar, 100 μm. Arrow indicated interlobular bile ducts.

(D-F) Immunohistochemical staining of Glut1 in non-tumorous liver tissues (N) and HCC tissues (T) in *AK* (D), *AKIDH1^{mut}* (E), and *AKIDH2^{mut}* (F) mice. Bar, 100 μm. Line showed the boundary between tumorous and non-tumorous area.

(G and H) Immunohistochemical staining of Glut1 in non-tumorous liver tissues (N) and ICC tissues (T) in AK*IDH1^{mut}* (G) and AK*IDH2^{mut}* (H) mice. Bar, 100 μm.

(I and J) Real time-PCR analysis of *Slc2a1* in non-tumorous tissues, HCC/DN tissues of *AKIDH1*^{mut} (I), and ICC tissues of *AKIDH2*^{mut} (J) mice (n=2). Expression of *Gapdh* was used as an internal control. The data represents mean ± SD from triplicate experiments. *** $p < 0.001$.

Discussion

In this study, I have shown that oncogenic *IDH1/2* mutations induce the expression of Glut1 *in vitro* and *in vivo*, and that activation of PI3K/AKT/mTOR pathway and up-regulation of Hif1α are involved in the induction of Glut1. In addition, I clarified that the *IDH1/2* mutations enhance the development of liver tumors, in particular ICC-like tumors, in the background of activating *Kras* mutation.

It is of note that the IDH2 mutant showed greater effects on the production of 2-HG *in vitro* compared with the IDH1 mutant. Regarding 2-HG production, similar observations were shown in previous reports[33, 66, 68]. Since IDH1 and IDH2 is a cytosolic and mitochondrial enzyme, respectively, IDH2 might have greater accessibility to α-KG than IDH1, resulting in a larger amount of 2-HG production. Consistent with this notion, it was reported that forced expression of mutant IDH1 that incorporated the N-terminal mitochondrial targeting sequence of IDH2 resulted in mitochondrial localization and greater accumulation of 2-HG in cells[68].

Unexpectedly, both IDH1 and IDH2 mutants inhibited cell proliferation in MEF cells. *IDH1* and *IDH2* were usually defined as atypical oncogenes for their double-edged sword role in human carcinogenesis[69-72]. Although *IDH* mutations had been reported to promote cell proliferation in many types of cancer cells as a basal oncogenic activity[4, 10], other studies also showed contradictory results of reduced cell growth induced by *IDH* mutations or 2-HG[73-76], suggesting that the effect of IDH mutants on cell proliferation is

dependent on different cell types. Interestingly, the GSEA analysis in the current study uncovered that genes associated with p53 pathway increased in MEF-2MUT cells (Table 5). This result suggests that activated p53 signaling pathway may be involved in the suppressed proliferation of MEF-2MUT cells. In addition, previous research had revealed that 2-HG can competitively bind and inhibit ATP synthase, resulting in decreased ATP contents, mitochondrial respiration and subsequent suppression of cell growth in *IDH1* mutant cells[77]. Wnt/β-catenin signaling was also clarified to be involved in the inhibition of cell proliferation, migration and invasion in *IDH1* mutant glioblastoma cell lines[75]. These studies indicated that repressed cell proliferation of MEF cells by IDH1/2 mutants might be correlated with a complex mechanism regulated by cell energy metabolism or signaling pathways.

In this study, I clarified that Glut1 encoded by *Slc2a1* is a *bona fide* downstream target of the *IDH* mutations. In addition to Glut1, I found that cyclooxygenase-2 (COX-2) encoded by *Ptgs2* and laminin gamma-2 encoded by *Lamc2* are candidate molecules regulated by the *IDH* mutations through the accumulation of 2-HG. It is of note that COX-2 has been reported to promote apoptotic resistance, proliferation, angiogenesis, inflammation, invasion, and metastasis of cancer cells[78]. Furthermore, COX-2 contributes to immune evasion and resistance to cancer immunotherapy[79]. On the other hand, laminin gamma-2, a laminin component, has been considered a specific marker for invasive and metastatic potential of tumors[80, 81]. Considering the pleiotropic and multifaceted roles of

COX-2 and laminin gamma-2 acting on tumorigenesis, the regulation of these two molecules by the *IDH1/2* mutations should be investigated in future studies.

Previous research reported that mutant IDH1 activates glycolysis through the upregulation of PFKP in mouse intrahepatic biliary organoid[82]. On the other hand, 2-HG attenuates aerobic glycolysis in leukemia by targeting the FTO/m^{6}A/PFKP/LDHB axis[83]. These studies indicate that the effect of *IDH* mutation or 2-HG on glucose metabolism may depend on cell type. Present study showed that the *IDH1/2* mutations induced altered glucose metabolism, enhanced glucose uptake and glycolysis, which is similar to the Warburg effect contributing in cancer cells[84]. Since mutant IDH1/2 enzymes convert α-KG into 2-HG, cancer cells carrying these mutants should have alterations in the concentration of TCA cycle intermediates, and require substitution of energy sources to attenuate the deficiency of metabolic substrates. It was suggested that lactate is actively imported and converted into α-KG in *IDH1* mutant gliomas, and that supplement of metabolic substrates is dependent on lactate, which are alleviating metabolic stress that results from defective isocitrate processing[85]. Therefore, increased Glut1 expression, glucose influx, and glycolysis by the *IDH1/2* mutations may function as a compensatory mechanism to rescue the aberrant aerobic respiration under the metabolic reprogramming. Additionally, *in vivo* evidence was also shown by this study that Glut1 expression is inclined to increase in ICC-like lesions of mice carrying liver-specific *IDH1/2* mutations. High levels of lactate dehydrogenase A, a key glycolytic enzyme catalyzing L-lactate generation, have been reported in ICC patients[86, 87]. Mutations in mitochondrial genes and

consequent impairment of oxidative phosphorylation were also suggested to be found in ICC tumors[27]. Collectively, these studies support the involvement of Warburg effect in ICC and indicate that enhanced expression of GLUT1 and consistent Warburg effect may play a crucial role in ICC tumorigenesis.

Elevated phosphorylation of S6k, Akt (Ser473) and Akt (Thr308) was detected in the MEF cells expressing IDH1/2 mutants, demonstrating the augmented activity of the PI3K/Akt/mTOR pathway. The underlying regulatory mechanism of Glut1 expression by *IDH* mutations-mediated PI3K/Akt/mTOR signaling was further investigated. Interestingly, reduced expression of Glut1 by pharmacological and genetic inhibition of the PI3K/Akt/mTORC1 pathway was demonstrated in this study. Several studies have reported that trafficking of GLUT1 to the cell surface was mediated through Akt activation[88-90]. Additionally, Akt activation was suggested to be associated with the gene expression of Glut1[91, 92]. Consistent with these reports, the data of present research indicated that activation of the PI3K/Akt/mTORC1 cascade by the *IDH* mutations transcriptionally upregulates Glut1 expression, and suggested the involvement of transcription factor(s).

HIF1α is a transcription factor that is correlated with metabolic alterations during tumorigenesis, and the protein is regulated through its degradation by prolyl hydroxylase (PHD)-mediated hydroxylation and subsequent hydroxylation-targeted ubiquitination under normoxic condition[93-95]. It has been reported that reduced α-KG level by conversion to 2-HG might increase the level of HIF1α, as α-KG is normally

necessary for PHD-mediated degradation of HIF1α[1, 69, 96]. However, other lines of evidence showed that 2-HG stimulates the activity of the PHD, which results in the decreased expression of HIF1α[97]. These studies remained the controversial mechanism (s) on how HIF1α is regulated in the context of *IDH* mutations. In the present study, RNA-seq revealed that *Hif1α* level was increased in MEF-2MUT cells compared to the control cells, indicating transcriptional upregulation of *Hif1α* by the *IDH2* mutation. Western blotting additionally showed that exogenous expression of the IDH1 or IDH2 mutant increased the Hif1α protein, and that knockdown of Hif1α reduced Glut1 expression in MEF-1MUT and MEF-2MUT cells. These data corroborated that Hif1α was also involved in the induction of Glut1 by the IDH1/2 mutants. Importantly, 2-HG treatment did not change the expression of *Hif1α* on mRNA level although Glut1 protein was induced by the treatment. This discrepancy may be explained by a report showing that Hif1α protein is stabilized by PHD inhibition in response to 2-HG[37]. In addition, previous studies demonstrated that mTOR activation regulates HIF1α expression by increased synthesis or stabilization of HIF1α[98-102]. Here, I corroborated that Hif1α expression is regulated by mTOR under the background of *IDH1/2* mutations.

Limitation of the present study includes the difference of cells utilized in this research. It is desirable to use normal epithelial cells instead of MEF or cancer cells for studying the function of *IDH1/2* mutations. Organoids established from liver tissues may be utilized as a substitute of normal epithelial cells in future studies.

In the mouse models, I clearly corroborated the increase of Glut1 in the non-tumorous liver and liver tumors in the oncogenic *IDH1/2* and *Kras* mutants double knockin mice. It is interesting that expression of Glut1 is higher in ICC-like tumors than HCC-like tumors. This may imply that dysregulation of glucose metabolism and accumulation of oncometabolites may be severer in the ICC-like tumors compared with the HCC-like tumors. The *in vitro* data in current study showed that expression of $IDH2^{R172S}$ produced larger amount of 2-HG than that of $IDH2^{R172S}$ in MEF cells. Consistent with this result, $AKIDH2^{mut}$ mice developed ICC-like tumors more frequently than $AKIDH1^{mut}$ mice, suggesting that increased 2-HG plays a crucial role in the development of ICC in the *Kras* mutant mice model. However, *IDH1* mutations are more frequently identified than *IDH2* in human ICCs (Figure 2), which uncovered the limitation of mimicking human malignancy using these mouse models. It has been reported that *Kras* is one of the most frequent mutations in ICCs and contributes to ICC tumorigenesis by stimulating cell proliferation together with other genetic deficiencies, such as *PTEN* or *TP53* mutations[27, 67]. Since a tendency of mutual exclusivity was observed between *IDH1* and *KRAS* mutations in human ICCs[49], other undetermined factors may influence the development of ICCs in IDH1 mutant cells more strongly than IDH2 mutant cells. Although I have reported here that $LSL\text{-}Kras^{G12D}$; $IDH2^{R172S}$ develops not only ICC but also HCC, Saha *et al.* previously reported that a liver-specific $LSL\text{-}Kras^{G12D}$; $IDH2^{R172K}$ knockin mouse developed ICC alone[103]. Compared with their mice maintained on a mixed 129SV/C57BL/6 background, the mice model in present study

was generated on a pure C57BL/6 background. The different genetic background may be associated with the difference of HCC development between the two mouse models. It is also possible that different mutations in *IDH2*, namely R172S in present study and R172K in Saha's study[103], may have distinct effect in hepatotumorigenesis in combination with oncogenic *Kras* mutation. It is of note that codon 172 is one of the two mutation hot spots in *IDH2*, and that codon 132 is the mutation hot spot in *IDH1*. The $IDH2^{R172S}$ mutation in ICC has been reported in an earlier report[25], and this mutation accounts for approximately 8% of mutations at codon 172 in biliary tract cancer according to the COSMIC database (https://cancer.sanger.ac.uk/cosmic). Additionally, COSMIC revealed that the $IDH1^{R132C}$ mutation accounts for approximately 64% of *IDH1* mutations at codon 132 in biliary tract cancer, and this mutation has been reported to be observed in 44% of ICC patients with *IDH1* mutations[25]. These data indicate the significance of these mouse models for understanding tumorigenesis of human ICC, especially the tumors harboring *IDH1* mutation.

Conclusion

In this study, RNA-seq analysis identified Glut1 as a target molecule induced by the oncogenic IDH1/2 mutants and 2-HG through the activation of PI3K/Akt/mTOR pathway and accumulation of Hif1α expression. Increased Glut1 expression consequently altered cellular glucose metabolism. Furthermore, liver-specific expression of the *IDH1/2* mutations enhanced the development of liver tumors especially that of ICC-like tumors in the background of oncogenic *Kras* mutation. These data may contribute to the understanding of molecular mechanisms underlying liver tumors with *IDH1/2* mutations, and the development of strategies to treat and/or prevent ICC.

References

1. Dang L, White DW, Gross S, Bennett BD, Bittinger MA, Driggers EM, Fantin VR, Jang HG, Jin S, Keenan MC, Marks KM, Prins RM, Ward PS, Yen KE, Liau LM, Rabinowitz JD, Cantley LC, Thompson CB, Vander Heiden MG, Su SM, Cancer-associated IDH1 mutations produce 2-hydroxyglutarate. *Nature* **462**, 739-44 (2009).
2. Yang H, Ye D, Guan KL, Xiong Y, IDH1 and IDH2 mutations in tumorigenesis: mechanistic insights and clinical perspectives. *Clin Cancer Res* **18**, 5562-71 (2012).
3. Dang L, Yen K, Attar EC, IDH mutations in cancer and progress toward development of targeted therapeutics. *Ann Oncol* **27**, 599-608 (2016).
4. Tommasini-Ghelfi S, Murnan K, Kouri FM, Mahajan AS, May JL, Stegh AH, Cancer-associated mutation and beyond: The emerging biology of isocitrate dehydrogenases in human disease. *Sci Adv* **5**, eaaw4543 (2019).
5. Cairns RA, Mak TW, Oncogenic isocitrate dehydrogenase mutations: mechanisms, models, and clinical opportunities. *Cancer Discov* **3**, 730-41 (2013).
6. Waitkus MS, Diplas BH, Yan H, Biological Role and Therapeutic Potential of IDH Mutations in Cancer. *Cancer Cell* **34**, 186-95 (2018).
7. Parsons DW, Jones S, Zhang X, Lin JC, Leary RJ, Angenendt P, Mankoo P,

Carter H, Siu IM, Gallia GL, Olivi A, McLendon R, Rasheed BA, Keir S, Nikolskaya T, Nikolsky Y, Busam DA, Tekleab H, Diaz LA, Hartigan J, Smith DR, Strausberg RL, Marie SK, Shinjo SM, Yan H, Riggins GJ, Bigner DD, Karchin R, Papadopoulos N, Parmigiani G, Vogelstein B, Velculescu VE, Kinzler KW, An integrated genomic analysis of human glioblastoma multiforme. *Science* **321**, 1807-12 (2008).

8. Yan H, Parsons DW, Jin G, McLendon R, Rasheed BA, Yuan W, Kos I, Batinic-Haberle I, Jones S, Riggins GJ, Friedman H, Friedman A, Reardon D, Herndon J, Kinzler KW, Velculescu VE, Vogelstein B, Bigner DD, IDH1 and IDH2 mutations in gliomas. *N Engl J Med* **360**, 765-73 (2009).

9. Reitman ZJ, Yan H, Isocitrate dehydrogenase 1 and 2 mutations in cancer: alterations at a crossroads of cellular metabolism. *J Natl Cancer Inst* **102**, 932-41 (2010).

10. Losman JA, Kaelin WG, What a difference a hydroxyl makes: mutant IDH, (R)-2-hydroxyglutarate, and cancer. *Genes Dev* **27**, 836-52 (2013).

11. M Gagné L, Boulay K, Topisirovic I, Huot M, Mallette FA, Oncogenic Activities of IDH1/2 Mutations: From Epigenetics to Cellular Signaling. *Trends Cell Biol* **27**, 738-52 (2017).

12. Clark O, Yen K, Mellinghoff IK, Molecular Pathways: Isocitrate Dehydrogenase Mutations in Cancer. *Clin Cancer Res* **22**, 1837-42 (2016).

13. Amary MF, Bacsi K, Maggiani F, Damato S, Halai D, Berisha F, Pollock R,

O'Donnell P, Grigoriadis A, Diss T, Eskandarpour M, Presneau N, Hogendoorn PC, Futreal A, Tirabosco R, Flanagan AM, IDH1 and IDH2 mutations are frequent events in central chondrosarcoma and central and periosteal chondromas but not in other mesenchymal tumours. *J Pathol* **224**, 334-43 (2011).

14. Pansuriya TC, van Eijk R, d'Adamo P, van Ruler MA, Kuijjer ML, Oosting J, Cleton-Jansen AM, van Oosterwijk JG, Verbeke SL, Meijer D, van Wezel T, Nord KH, Sangiorgi L, Toker B, Liegl-Atzwanger B, San-Julian M, Sciot R, Limaye N, Kindblom LG, Daugaard S, Godfraind C, Boon LM, Vikkula M, Kurek KC, Szuhai K, French PJ, Bovée JV, Somatic mosaic IDH1 and IDH2 mutations are associated with enchondroma and spindle cell hemangioma in Ollier disease and Maffucci syndrome. *Nat Genet* **43**, 1256-61 (2011).

15. Mardis ER, Ding L, Dooling DJ, Larson DE, McLellan MD, Chen K, Koboldt DC, Fulton RS, Delehaunty KD, McGrath SD, Fulton LA, Locke DP, Magrini VJ, Abbott RM, Vickery TL, Reed JS, Robinson JS, Wylie T, Smith SM, Carmichael L, Eldred JM, Harris CC, Walker J, Peck JB, Du F, Dukes AF, Sanderson GE, Brummett AM, Clark E, McMichael JF, Meyer RJ, Schindler JK, Pohl CS, Wallis JW, Shi X, Lin L, Schmidt H, Tang Y, Haipek C, Wiechert ME, Ivy JV, Kalicki J, Elliott G, Ries RE, Payton JE, Westervelt P, Tomasson MH, Watson MA, Baty J, Heath S, Shannon WD, Nagarajan R, Link DC, Walter MJ, Graubert TA, DiPersio JF, Wilson RK, Ley TJ, Recurring mutations found by

sequencing an acute myeloid leukemia genome. *N Engl J Med* **361**, 1058-66 (2009).

16. Ward PS, Patel J, Wise DR, Abdel-Wahab O, Bennett BD, Coller HA, Cross JR, Fantin VR, Hedvat CV, Perl AE, Rabinowitz JD, Carroll M, Su SM, Sharp KA, Levine RL, Thompson CB, The common feature of leukemia-associated IDH1 and IDH2 mutations is a neomorphic enzyme activity converting alpha-ketoglutarate to 2-hydroxyglutarate. *Cancer Cell* **17**, 225-34 (2010).

17. Ohgaki H, Kleihues P, The definition of primary and secondary glioblastoma. *Clin Cancer Res* **19**, 764-72 (2013).

18. Mondesir J, Willekens C, Touat M, de Botton S, IDH1 and IDH2 mutations as novel therapeutic targets: current perspectives. *J Blood Med* **7**, 171-80 (2016).

19. Hartmann C, Meyer J, Balss J, Capper D, Mueller W, Christians A, Felsberg J, Wolter M, Mawrin C, Wick W, Weller M, Herold-Mende C, Unterberg A, Jeuken JW, Wesseling P, Reifenberger G, von Deimling A, Type and frequency of IDH1 and IDH2 mutations are related to astrocytic and oligodendroglial differentiation and age: a study of 1,010 diffuse gliomas. *Acta Neuropathol* **118**, 469-74 (2009).

20. Im AP, Sehgal AR, Carroll MP, Smith BD, Tefferi A, Johnson DE, Boyiadzis M, DNMT3A and IDH mutations in acute myeloid leukemia and other myeloid malignancies: associations with prognosis and potential treatment strategies. *Leukemia* **28**, 1774-83 (2014).

21. Chou WC, Lei WC, Ko BS, Hou HA, Chen CY, Tang JL, Yao M, Tsay W, Wu

SJ, Huang SY, Hsu SC, Chen YC, Chang YC, Kuo KT, Lee FY, Liu MC, Liu CW, Tseng MH, Huang CF, Tien HF, The prognostic impact and stability of Isocitrate dehydrogenase 2 mutation in adult patients with acute myeloid leukemia. *Leukemia* **25**, 246-53 (2011).

22. Abbas S, Lugthart S, Kavelaars FG, Schelen A, Koenders JE, Zeilemaker A, van Putten WJ, Rijneveld AW, Löwenberg B, Valk PJ, Acquired mutations in the genes encoding IDH1 and IDH2 both are recurrent aberrations in acute myeloid leukemia: prevalence and prognostic value. *Blood* **116**, 2122-6 (2010).

23. Borger DR, Tanabe KK, Fan KC, Lopez HU, Fantin VR, Straley KS, Schenkein DP, Hezel AF, Ancukiewicz M, Liebman HM, Kwak EL, Clark JW, Ryan DP, Deshpande V, Dias-Santagata D, Ellisen LW, Zhu AX, Iafrate AJ, Frequent mutation of isocitrate dehydrogenase (IDH)1 and IDH2 in cholangiocarcinoma identified through broad-based tumor genotyping. *Oncologist* **17**, 72-9 (2012).

24. Wang P, Dong Q, Zhang C, Kuan PF, Liu Y, Jeck WR, Andersen JB, Jiang W, Savich GL, Tan TX, Auman JT, Hoskins JM, Misher AD, Moser CD, Yourstone SM, Kim JW, Cibulskis K, Getz G, Hunt HV, Thorgeirsson SS, Roberts LR, Ye D, Guan KL, Xiong Y, Qin LX, Chiang DY, Mutations in isocitrate dehydrogenase 1 and 2 occur frequently in intrahepatic cholangiocarcinomas and share hypermethylation targets with glioblastomas. *Oncogene* **32**, 3091-100 (2013).

25. Grassian AR, Pagliarini R, Chiang DY, Mutations of isocitrate dehydrogenase 1

and 2 in intrahepatic cholangiocarcinoma. *Curr Opin Gastroenterol* **30**, 295-302 (2014).

26. Kipp BR, Voss JS, Kerr SE, Barr Fritcher EG, Graham RP, Zhang L, Highsmith WE, Zhang J, Roberts LR, Gores GJ, Halling KC, Isocitrate dehydrogenase 1 and 2 mutations in cholangiocarcinoma. *Hum Pathol* **43**, 1552-8 (2012).

27. Zou S, Li J, Zhou H, Frech C, Jiang X, Chu JS, Zhao X, Li Y, Li Q, Wang H, Hu J, Kong G, Wu M, Ding C, Chen N, Hu H, Mutational landscape of intrahepatic cholangiocarcinoma. *Nat Commun* **5**, 5696 (2014).

28. Jiao Y, Pawlik TM, Anders RA, Selaru FM, Streppel MM, Lucas DJ, Niknafs N, Guthrie VB, Maitra A, Argani P, Offerhaus GJA, Roa JC, Roberts LR, Gores GJ, Popescu I, Alexandrescu ST, Dima S, Fassan M, Simbolo M, Mafficini A, Capelli P, Lawlor RT, Ruzzenente A, Guglielmi A, Tortora G, de Braud F, Scarpa A, Jarnagin W, Klimstra D, Karchin R, Velculescu VE, Hruban RH, Vogelstein B, Kinzler KW, Papadopoulos N, Wood LD, Exome sequencing identifies frequent inactivating mutations in BAP1, ARID1A and PBRM1 in intrahepatic cholangiocarcinomas. *Nat Genet* **45**, 1470-3 (2013).

29. Al-Khallaf H, Isocitrate dehydrogenases in physiology and cancer: biochemical and molecular insight. *Cell Biosci* **7**, 37 (2017).

30. Gupta R, Flanagan S, Li CC, Lee M, Shivalingham B, Maleki S, Wheeler HR, Buckland ME, Expanding the spectrum of IDH1 mutations in gliomas. *Mod Pathol* **26**, 619-25 (2013).

31. Marcucci G, Maharry K, Wu YZ, Radmacher MD, Mrózek K, Margeson D, Holland KB, Whitman SP, Becker H, Schwind S, Metzeler KH, Powell BL, Carter TH, Kolitz JE, Wetzler M, Carroll AJ, Baer MR, Caligiuri MA, Larson RA, Bloomfield CD, IDH1 and IDH2 gene mutations identify novel molecular subsets within de novo cytogenetically normal acute myeloid leukemia: a Cancer and Leukemia Group B study. *J Clin Oncol* **28**, 2348-55 (2010).

32. Lu C, Ward PS, Kapoor GS, Rohle D, Turcan S, Abdel-Wahab O, Edwards CR, Khanin R, Figueroa ME, Melnick A, Wellen KE, O'Rourke DM, Berger SL, Chan TA, Levine RL, Mellinghoff IK, Thompson CB, IDH mutation impairs histone demethylation and results in a block to cell differentiation. *Nature* **483**, 474-8 (2012).

33. Figueroa ME, Abdel-Wahab O, Lu C, Ward PS, Patel J, Shih A, Li Y, Bhagwat N, Vasanthakumar A, Fernandez HF, Tallman MS, Sun Z, Wolniak K, Peeters JK, Liu W, Choe SE, Fantin VR, Paietta E, Löwenberg B, Licht JD, Godley LA, Delwel R, Valk PJ, Thompson CB, Levine RL, Melnick A, Leukemic IDH1 and IDH2 mutations result in a hypermethylation phenotype, disrupt TET2 function, and impair hematopoietic differentiation. *Cancer Cell* **18**, 553-67 (2010).

34. Sulkowski PL, Corso CD, Robinson ND, Scanlon SE, Purshouse KR, Bai H, Liu Y, Sundaram RK, Hegan DC, Fons NR, Breuer GA, Song Y, Mishra-Gorur K, De Feyter HM, de Graaf RA, Surovtseva YV, Kachman M, Halene S, Günel M, Glazer PM, Bindra RS, 2-Hydroxyglutarate produced by neomorphic IDH

mutations suppresses homologous recombination and induces PARP inhibitor sensitivity. *Sci Transl Med* **9**, (2017).

35. Molenaar RJ, Radivoyevitch T, Maciejewski JP, van Noorden CJ, Bleeker FE, The driver and passenger effects of isocitrate dehydrogenase 1 and 2 mutations in oncogenesis and survival prolongation. *Biochim Biophys Acta* **1846**, 326-41 (2014).

36. Han S, Liu Y, Cai SJ, Qian M, Ding J, Larion M, Gilbert MR, Yang C, IDH mutation in glioma: molecular mechanisms and potential therapeutic targets. *Br J Cancer* **122**, 1580-9 (2020).

37. Xu W, Yang H, Liu Y, Yang Y, Wang P, Kim SH, Ito S, Yang C, Xiao MT, Liu LX, Jiang WQ, Liu J, Zhang JY, Wang B, Frye S, Zhang Y, Xu YH, Lei QY, Guan KL, Zhao SM, Xiong Y, Oncometabolite 2-hydroxyglutarate is a competitive inhibitor of α-ketoglutarate-dependent dioxygenases. *Cancer Cell* **19**, 17-30 (2011).

38. Prensner JR, Chinnaiyan AM, Metabolism unhinged: IDH mutations in cancer. *Nat Med* **17**, 291-3 (2011).

39. Chowdhury R, Yeoh KK, Tian YM, Hillringhaus L, Bagg EA, Rose NR, Leung IK, Li XS, Woon EC, Yang M, McDonough MA, King ON, Clifton IJ, Klose RJ, Claridge TD, Ratcliffe PJ, Schofield CJ, Kawamura A, The oncometabolite 2-hydroxyglutarate inhibits histone lysine demethylases. *EMBO Rep* **12**, 463-9 (2011).

40. Nakamura H, Arai Y, Totoki Y, Shirota T, Elzawahry A, Kato M, Hama N, Hosoda F, Urushidate T, Ohashi S, Hiraoka N, Ojima H, Shimada K, Okusaka T, Kosuge T, Miyagawa S, Shibata T, Genomic spectra of biliary tract cancer. *Nat Genet* **47**, 1003-10 (2015).

41. Blechacz B, Cholangiocarcinoma: Current Knowledge and New Developments. *Gut Liver* **11**, 13-26 (2017).

42. Hoyos S, Navas MC, Restrepo JC, Botero RC, Current controversies in cholangiocarcinoma. *Biochim Biophys Acta Mol Basis Dis* **1864**, 1461-7 (2018).

43. Razumilava N, Gores GJ, Cholangiocarcinoma. *Lancet* **383**, 2168-79 (2014).

44. Rizvi S, Khan SA, Hallemeier CL, Kelley RK, Gores GJ, Cholangiocarcinoma - evolving concepts and therapeutic strategies. *Nat Rev Clin Oncol* **15**, 95-111 (2018).

45. Banales JM, Marin JJG, Lamarca A, Rodrigues PM, Khan SA, Roberts LR, Cardinale V, Carpino G, Andersen JB, Braconi C, Calvisi DF, Perugorria MJ, Fabris L, Boulter L, Macias RIR, Gaudio E, Alvaro D, Gradilone SA, Strazzabosco M, Marzioni M, Coulouarn C, Fouassier L, Raggi C, Invernizzi P, Mertens JC, Moncsek A, Rizvi S, Heimbach J, Koerkamp BG, Bruix J, Forner A, Bridgewater J, Valle JW, Gores GJ, Cholangiocarcinoma 2020: the next horizon in mechanisms and management. *Nat Rev Gastroenterol Hepatol* **17**, 557-88 (2020).

46. Brown KM, Parmar AD, Geller DA, Intrahepatic cholangiocarcinoma. *Surg*

Oncol Clin N Am **23**, 231-46 (2014).

47. Buettner S, van Vugt JL, IJzermans JN, Groot Koerkamp B, Intrahepatic cholangiocarcinoma: current perspectives. *Onco Targets Ther* **10**, 1131-42 (2017).

48. Ross JS, Wang K, Gay L, Al-Rohil R, Rand JV, Jones DM, Lee HJ, Sheehan CE, Otto GA, Palmer G, Yelensky R, Lipson D, Morosini D, Hawryluk M, Catenacci DV, Miller VA, Churi C, Ali S, Stephens PJ, New routes to targeted therapy of intrahepatic cholangiocarcinomas revealed by next-generation sequencing. *Oncologist* **19**, 235-42 (2014).

49. Lowery MA, Ptashkin R, Jordan E, Berger MF, Zehir A, Capanu M, Kemeny NE, O'Reilly EM, El-Dika I, Jarnagin WR, Harding JJ, D'Angelica MI, Cercek A, Hechtman JF, Solit DB, Schultz N, Hyman DM, Klimstra DS, Saltz LB, Abou-Alfa GK, Comprehensive Molecular Profiling of Intrahepatic and Extrahepatic Cholangiocarcinomas: Potential Targets for Intervention. *Clin Cancer Res* **24**, 4154-61 (2018).

50. Lee K, Song YS, Shin Y, Wen X, Kim Y, Cho NY, Bae JM, Kang GH, Intrahepatic cholangiocarcinomas with IDH1/2 mutation-associated hypermethylation at selective genes and their clinicopathological features. *Sci Rep* **10**, 15820 (2020).

51. Goyal L, Govindan A, Sheth RA, Nardi V, Blaszkowsky LS, Faris JE, Clark JW, Ryan DP, Kwak EL, Allen JN, Murphy JE, Saha SK, Hong TS, Wo JY, Ferrone

CR, Tanabe KK, Chong DQ, Deshpande V, Borger DR, Iafrate AJ, Bardeesy N, Zheng H, Zhu AX, Prognosis and Clinicopathologic Features of Patients With Advanced Stage Isocitrate Dehydrogenase (IDH) Mutant and IDH Wild-Type Intrahepatic Cholangiocarcinoma. *Oncologist* **20**, 1019-27 (2015).

52. Zhu AX, Borger DR, Kim Y, Cosgrove D, Ejaz A, Alexandrescu S, Groeschl RT, Deshpande V, Lindberg JM, Ferrone C, Sempoux C, Yau T, Poon R, Popescu I, Bauer TW, Gamblin TC, Gigot JF, Anders RA, Pawlik TM, Genomic profiling of intrahepatic cholangiocarcinoma: refining prognosis and identifying therapeutic targets. *Ann Surg Oncol* **21**, 3827-34 (2014).

53. Hanahan D, Weinberg RA, Hallmarks of cancer: the next generation. *Cell* **144**, 646-74 (2011).

54. Adekola K, Rosen ST, Shanmugam M, Glucose transporters in cancer metabolism. *Curr Opin Oncol* **24**, 650-4 (2012).

55. Chen C, Pore N, Behrooz A, Ismail-Beigi F, Maity A, Regulation of glut1 mRNA by hypoxia-inducible factor-1. Interaction between H-ras and hypoxia. *J Biol Chem* **276**, 9519-25 (2001).

56. Hayashi M, Sakata M, Takeda T, Yamamoto T, Okamoto Y, Sawada K, Kimura A, Minekawa R, Tahara M, Tasaka K, Murata Y, Induction of glucose transporter 1 expression through hypoxia-inducible factor 1alpha under hypoxic conditions in trophoblast-derived cells. *J Endocrinol* **183**, 145-54 (2004).

57. Wieman HL, Wofford JA, Rathmell JC, Cytokine stimulation promotes glucose

uptake via phosphatidylinositol-3 kinase/Akt regulation of Glut1 activity and trafficking. *Mol Biol Cell* **18**, 1437-46 (2007).

58. Jacobs SR, Herman CE, Maciver NJ, Wofford JA, Wieman HL, Hammen JJ, Rathmell JC, Glucose uptake is limiting in T cell activation and requires CD28-mediated Akt-dependent and independent pathways. *J Immunol* **180**, 4476-86 (2008).

59. Fang J, Zhou SH, Fan J, Yan SX, Roles of glucose transporter-1 and the phosphatidylinositol 3-kinase/protein kinase B pathway in cancer radioresistance (review). *Mol Med Rep* **11**, 1573-81 (2015).

60. Zhang Z, Yao L, Yang J, Wang Z, Du G, PI3K/Akt and HIF-1 signaling pathway in hypoxia-ischemia (Review). *Mol Med Rep* **18**, 3547-54 (2018).

61. Carvalho KC, Cunha IW, Rocha RM, Ayala FR, Cajaíba MM, Begnami MD, Vilela RS, Paiva GR, Andrade RG, Soares FA, GLUT1 expression in malignant tumors and its use as an immunodiagnostic marker. *Clinics (Sao Paulo)* **66**, 965-72 (2011).

62. Zambrano A, Molt M, Uribe E, Salas M, Glut 1 in Cancer Cells and the Inhibitory Action of Resveratrol as A Potential Therapeutic Strategy. *Int J Mol Sci* **20**, (2019).

63. Ancey PB, Contat C, Meylan E, Glucose transporters in cancer - from tumor cells to the tumor microenvironment. *FEBS J* **285**, 2926-43 (2018).

64. Kubo Y, Aishima S, Tanaka Y, Shindo K, Mizuuchi Y, Abe K, Shirabe K,

Maehara Y, Honda H, Oda Y, Different expression of glucose transporters in the progression of intrahepatic cholangiocarcinoma. *Hum Pathol* **45**, 1610-7 (2014).

65. Paudyal B, Oriuchi N, Paudyal P, Higuchi T, Nakajima T, Endo K, Expression of glucose transporters and hexokinase II in cholangiocellular carcinoma compared using [18F]-2-fluro-2-deoxy-D-glucose positron emission tomography. *Cancer Sci* **99**, 260-6 (2008).

66. Carbonneau M, M Gagné L, Lalonde ME, Germain MA, Motorina A, Guiot MC, Secco B, Vincent EE, Tumber A, Hulea L, Bergeman J, Oppermann U, Jones RG, Laplante M, Topisirovic I, Petrecca K, Huot M, Mallette FA, The oncometabolite 2-hydroxyglutarate activates the mTOR signalling pathway. *Nat Commun* **7**, 12700 (2016).

67. Ikenoue T, Terakado Y, Nakagawa H, Hikiba Y, Fujii T, Matsubara D, Noguchi R, Zhu C, Yamamoto K, Kudo Y, Asaoka Y, Yamaguchi K, Ijichi H, Tateishi K, Fukushima N, Maeda S, Koike K, Furukawa Y, A novel mouse model of intrahepatic cholangiocarcinoma induced by liver-specific Kras activation and Pten deletion. *Sci Rep* **6**, 23899 (2016).

68. Ward PS, Lu C, Cross JR, Abdel-Wahab O, Levine RL, Schwartz GK, Thompson CB, The potential for isocitrate dehydrogenase mutations to produce 2-hydroxyglutarate depends on allele specificity and subcellular compartmentalization. *J Biol Chem* **288**, 3804-15 (2013).

69. Zhao S, Lin Y, Xu W, Jiang W, Zha Z, Wang P, Yu W, Li Z, Gong L, Peng Y,

Ding J, Lei Q, Guan KL, Xiong Y, Glioma-derived mutations in IDH1 dominantly inhibit IDH1 catalytic activity and induce HIF-1alpha. *Science* **324**, 261-5 (2009).

70. Calvert AE, Chalastanis A, Wu Y, Hurley LA, Kouri FM, Bi Y, Kachman M, May JL, Bartom E, Hua Y, Mishra RK, Schiltz GE, Dubrovskyi O, Mazar AP, Peter ME, Zheng H, James CD, Burant CF, Chandel NS, Davuluri RV, Horbinski C, Stegh AH, Cancer-Associated IDH1 Promotes Growth and Resistance to Targeted Therapies in the Absence of Mutation. *Cell Rep* **19**, 1858-73 (2017).

71. Su R, Dong L, Li C, Nachtergaele S, Wunderlich M, Qing Y, Deng X, Wang Y, Weng X, Hu C, Yu M, Skibbe J, Dai Q, Zou D, Wu T, Yu K, Weng H, Huang H, Ferchen K, Qin X, Zhang B, Qi J, Sasaki AT, Plas DR, Bradner JE, Wei M, Marcucci G, Jiang X, Mulloy JC, Jin J, He C, Chen J, R-2HG Exhibits Anti-tumor Activity by Targeting FTO/m. *Cell* **172**, 90-105.e23 (2018).

72. Núñez FJ, Mendez FM, Kadiyala P, Alghamri MS, Savelieff MG, Garcia-Fabiani MB, Haase S, Koschmann C, Calinescu AA, Kamran N, Saxena M, Patel R, Carney S, Guo MZ, Edwards M, Ljungman M, Qin T, Sartor MA, Tagett R, Venneti S, Brosnan-Cashman J, Meeker A, Gorbunova V, Zhao L, Kremer DM, Zhang L, Lyssiotis CA, Jones L, Herting CJ, Ross JL, Hambardzumyan D, Hervey-Jumper S, Figueroa ME, Lowenstein PR, Castro MG, IDH1-R132H acts as a tumor suppressor in glioma via epigenetic up-regulation of the DNA damage response. *Sci Transl Med* **11**, (2019).

73. Bralten LB, Kloosterhof NK, Balvers R, Sacchetti A, Lapre L, Lamfers M, Leenstra S, de Jonge H, Kros JM, Jansen EE, Struys EA, Jakobs C, Salomons GS, Diks SH, Peppelenbosch M, Kremer A, Hoogenraad CC, Smitt PA, French PJ, IDH1 R132H decreases proliferation of glioma cell lines in vitro and in vivo. *Ann Neurol* **69**, 455-63 (2011).

74. Nie QM, Lin YY, Yang X, Shen L, Guo LM, Que SL, Li XX, Ge JW, Wang GS, Xiong WH, Guo P, Qiu YM, IDH1R^{132}H decreases the proliferation of U87 glioma cells through upregulation of microRNA-128a. *Mol Med Rep* **12**, 6695-701 (2015).

75. Cui D, Ren J, Shi J, Feng L, Wang K, Zeng T, Jin Y, Gao L, R132H mutation in IDH1 gene reduces proliferation, cell survival and invasion of human glioma by downregulating Wnt/β-catenin signaling. *Int J Biochem Cell Biol* **73**, 72-81 (2016).

76. Bunse L, Pusch S, Bunse T, Sahm F, Sanghvi K, Friedrich M, Alansary D, Sonner JK, Green E, Deumelandt K, Kilian M, Neftel C, Uhlig S, Kessler T, von Landenberg A, Berghoff AS, Marsh K, Steadman M, Zhu D, Nicolay B, Wiestler B, Breckwoldt MO, Al-Ali R, Karcher-Bausch S, Bozza M, Oezen I, Kramer M, Meyer J, Habel A, Eisel J, Poschet G, Weller M, Preusser M, Nadji-Ohl M, Thon N, Burger MC, Harter PN, Ratliff M, Harbottle R, Benner A, Schrimpf D, Okun J, Herold-Mende C, Turcan S, Kaulfuss S, Hess-Stumpp H, Bieback K, Cahill DP, Plate KH, Hänggi D, Dorsch M, Suvà ML, Niemeyer BA, von Deimling A,

Wick W, Platten M, Suppression of antitumor T cell immunity by the oncometabolite (R)-2-hydroxyglutarate. *Nat Med* **24**, 1192-203 (2018).

77. Fu X, Chin RM, Vergnes L, Hwang H, Deng G, Xing Y, Pai MY, Li S, Ta L, Fazlollahi F, Chen C, Prins RM, Teitell MA, Nathanson DA, Lai A, Faull KF, Jiang M, Clarke SG, Cloughesy TF, Graeber TG, Braas D, Christofk HR, Jung ME, Reue K, Huang J, 2-Hydroxyglutarate Inhibits ATP Synthase and mTOR Signaling. *Cell Metab* **22**, 508-15 (2015).

78. Hashemi Goradel N, Najafi M, Salehi E, Farhood B, Mortezaee K, Cyclooxygenase-2 in cancer: A review. *J Cell Physiol* **234**, 5683-99 (2019).

79. Liu B, Qu L, Yan S, Cyclooxygenase-2 promotes tumor growth and suppresses tumor immunity. *Cancer Cell Int* **15**, 106 (2015).

80. Garg M, Braunstein G, Koeffler HP, LAMC2 as a therapeutic target for cancers. *Expert Opin Ther Targets* **18**, 979-82 (2014).

81. Moon YW, Rao G, Kim JJ, Shim HS, Park KS, An SS, Kim B, Steeg PS, Sarfaraz S, Changwoo Lee L, Voeller D, Choi EY, Luo J, Palmieri D, Chung HC, Kim JH, Wang Y, Giaccone G, LAMC2 enhances the metastatic potential of lung adenocarcinoma. *Cell Death Differ* **22**, 1341-52 (2015).

82. Fujiwara H, Tateishi K, Misumi K, Hayashi A, Igarashi K, Kato H, Nakatsuka T, Suzuki N, Yamamoto K, Kudo Y, Hayakawa Y, Nakagawa H, Tanaka Y, Ijichi H, Kogure H, Nakai Y, Isayama H, Hasegawa K, Fukayama M, Soga T, Koike K, Mutant IDH1 confers resistance to energy stress in normal biliary cells

through PFKP-induced aerobic glycolysis and AMPK activation. *Sci Rep* **9**, 18859 (2019).

83. Qing Y, Dong L, Gao L, Li C, Li Y, Han L, Prince E, Tan B, Deng X, Wetzel C, Shen C, Gao M, Chen Z, Li W, Zhang B, Braas D, Ten Hoeve J, Sanchez GJ, Chen H, Chan LN, Chen CW, Ann D, Jiang L, Muschen M, Marcucci G, Plas DR, Li Z, Su R, Chen J, R-2-hydroxyglutarate attenuates aerobic glycolysis in leukemia by targeting the FTO/m(6)A/PFKP/LDHB axis. *Mol Cell* (2021).

84. Liberti MV, Locasale JW, The Warburg Effect: How Does it Benefit Cancer Cells? *Trends Biochem Sci* **41**, 211-8 (2016).

85. Lenting K, Khurshed M, Peeters TH, van den Heuvel CNAM, van Lith SAM, de Bitter T, Hendriks W, Span PN, Molenaar RJ, Botman D, Verrijp K, Heerschap A, Ter Laan M, Kusters B, van Ewijk A, Huynen MA, van Noorden CJF, Leenders WPJ, Isocitrate dehydrogenase 1-mutated human gliomas depend on lactate and glutamate to alleviate metabolic stress. *FASEB J* **33**, 557-71 (2019).

86. Yu Y, Liao M, Liu R, Chen J, Feng H, Fu Z, Overexpression of lactate dehydrogenase-A in human intrahepatic cholangiocarcinoma: its implication for treatment. *World J Surg Oncol* **12**, 78 (2014).

87. Thonsri U, Seubwai W, Waraasawapati S, Sawanyawisuth K, Vaeteewoottacharn K, Boonmars T, Cha'on U, Overexpression of lactate dehydrogenase A in cholangiocarcinoma is correlated with poor prognosis.

Histol Histopathol **32**, 503-10 (2017).

88. Siska PJ, van der Windt GJ, Kishton RJ, Cohen S, Eisner W, MacIver NJ, Kater AP, Weinberg JB, Rathmell JC, Suppression of Glut1 and Glucose Metabolism by Decreased Akt/mTORC1 Signaling Drives T Cell Impairment in B Cell Leukemia. *J Immunol* **197**, 2532-40 (2016).

89. Hoxhaj G, Manning BD, The PI3K-AKT network at the interface of oncogenic signalling and cancer metabolism. *Nat Rev Cancer* **20**, 74-88 (2020).

90. Rathmell JC, Fox CJ, Plas DR, Hammerman PS, Cinalli RM, Thompson CB, Akt-directed glucose metabolism can prevent Bax conformation change and promote growth factor-independent survival. *Mol Cell Biol* **23**, 7315-28 (2003).

91. Barthel A, Okino ST, Liao J, Nakatani K, Li J, Whitlock JP, Roth RA, Regulation of GLUT1 gene transcription by the serine/threonine kinase Akt1. *J Biol Chem* **274**, 20281-6 (1999).

92. Plas DR, Talapatra S, Edinger AL, Rathmell JC, Thompson CB, Akt and Bcl-xL promote growth factor-independent survival through distinct effects on mitochondrial physiology. *J Biol Chem* **276**, 12041-8 (2001).

93. Bruick RK, McKnight SL, A conserved family of prolyl-4-hydroxylases that modify HIF. *Science* **294**, 1337-40 (2001).

94. Epstein AC, Gleadle JM, McNeill LA, Hewitson KS, O'Rourke J, Mole DR, Mukherji M, Metzen E, Wilson MI, Dhanda A, Tian YM, Masson N, Hamilton DL, Jaakkola P, Barstead R, Hodgkin J, Maxwell PH, Pugh CW, Schofield CJ,

Ratcliffe PJ, C. elegans EGL-9 and mammalian homologs define a family of dioxygenases that regulate HIF by prolyl hydroxylation. *Cell* **107**, 43-54 (2001).

95. Jaakkola P, Mole DR, Tian YM, Wilson MI, Gielbert J, Gaskell SJ, von Kriegsheim A, Hebestreit HF, Mukherji M, Schofield CJ, Maxwell PH, Pugh CW, Ratcliffe PJ, Targeting of HIF-alpha to the von Hippel-Lindau ubiquitylation complex by O2-regulated prolyl hydroxylation. *Science* **292**, 468-72 (2001).

96. Majmundar AJ, Wong WJ, Simon MC, Hypoxia-inducible factors and the response to hypoxic stress. *Mol Cell* **40**, 294-309 (2010).

97. Koivunen P, Lee S, Duncan CG, Lopez G, Lu G, Ramkissoon S, Losman JA, Joensuu P, Bergmann U, Gross S, Travins J, Weiss S, Looper R, Ligon KL, Verhaak RG, Yan H, Kaelin WG, Transformation by the (R)-enantiomer of 2-hydroxyglutarate linked to EGLN activation. *Nature* **483**, 484-8 (2012).

98. Düvel K, Yecies JL, Menon S, Raman P, Lipovsky AI, Souza AL, Triantafellow E, Ma Q, Gorski R, Cleaver S, Vander Heiden MG, MacKeigan JP, Finan PM, Clish CB, Murphy LO, Manning BD, Activation of a metabolic gene regulatory network downstream of mTOR complex 1. *Mol Cell* **39**, 171-83 (2010).

99. Tandon P, Gallo CA, Khatri S, Barger JF, Yepiskoposyan H, Plas DR, Requirement for ribosomal protein S6 kinase 1 to mediate glycolysis and apoptosis resistance induced by Pten deficiency. *Proc Natl Acad Sci U S A* **108**, 2361-5 (2011).

100. Dodd KM, Yang J, Shen MH, Sampson JR, Tee AR, mTORC1 drives HIF-1α and VEGF-A signalling via multiple mechanisms involving 4E-BP1, S6K1 and STAT3. *Oncogene* **34**, 2239-50 (2015).

101. He L, Gomes AP, Wang X, Yoon SO, Lee G, Nagiec MJ, Cho S, Chavez A, Islam T, Yu Y, Asara JM, Kim BY, Blenis J, mTORC1 Promotes Metabolic Reprogramming by the Suppression of GSK3-Dependent Foxk1 Phosphorylation. *Mol Cell* **70**, 949-60.e4 (2018).

102. Hudson CC, Liu M, Chiang GG, Otterness DM, Loomis DC, Kaper F, Giaccia AJ, Abraham RT, Regulation of hypoxia-inducible factor 1alpha expression and function by the mammalian target of rapamycin. *Mol Cell Biol* **22**, 7004-14 (2002).

103. Saha SK, Parachoniak CA, Ghanta KS, Fitamant J, Ross KN, Najem MS, Gurumurthy S, Akbay EA, Sia D, Cornella H, Miltiadous O, Walesky C, Deshpande V, Zhu AX, Hezel AF, Yen KE, Straley KS, Travins J, Popovici-Muller J, Gliser C, Ferrone CR, Apte U, Llovet JM, Wong KK, Ramaswamy S, Bardeesy N, Mutant IDH inhibits HNF-4α to block hepatocyte differentiation and promote biliary cancer. *Nature* **513**, 110-4 (2014).

Acknowledgements

I would like to express my gratitude to all those who helped me writing this thesis.

I gratefully acknowledge the help of my supervisor, Professor Yoichi Furukawa, who has offered me valuable suggestions in the academic studies. Without his patient instruction, insightful criticism and expert guidance, the completion of this thesis would not have been possible.

I also gratefully acknowledge the help of my supervisor, Associate Professor Tsuneo Ikenoue, who has given me so much advice and encouragement on my research and this thesis.

I am also deeply indebted to Dr. Kiyoshi Yamaguchi, Seira Hatakeyama, Yumiko Isobe, Rika Koubo and the laboratory members in Division of Clinical Genome Research, The Institute of Medical Science, The University of Tokyo, for their kind help and encouragement to me during my research.

Finally, I should express my very profound gratitude to my family for giving me unfailing support and continuous encouragement throughout my years of study and through the process of writing this thesis.